The Role of *TRF4* in the Maintenance of CAG Repeats in Yeast

An honors thesis for the Department of Biology

Lauren Verra

Tufts University, 2010

Abstract

Trinucleotide repeats are repetitive sequences in the genome prone to both fragility and instability. The *Saccharomyces cerevisiae* gene *TRF4* may function in DNA repair or cohesion mechanisms, in addition to an RNA-level role leading to the degradation of aberrant RNAs. This study shows that Δ*trf4* displays increased fragility and instability in CAG repeat tracts over wild-type yeast, suggesting a role for *TRF4* in the maintenance of CAG repeats in the genome. In contrast, the mutant for *TRF4*'s homologue *TRF5* displays no increased repeat fragility or instability over the wild-type. In order to further understand *TRF4*'s potential role in maintenance of CAG repeats, genetic experiments were performed to determine whether this phenotype can be attributed to a role of *TRF4* in double-stranded break repair, the potential fork stabilization pathway of the Ctf18 replication factor C-like complex, or post-replication repair.

Introduction

Trinucleotide repeats (TNRs) are repetitive sequences within the genome. Expansions of TNRs cause several human genetic diseases (Freudenreich & Lahiri 2004). Of particular importance is the CAG/CTG repeat, which is involved in 12 inherited diseases, including Huntington's disease, several types of spinocerebellar ataxia, myotonic dystrophy, and Kennedy's disease (Freudenreich & Lahiri 2004). CAG repeat tracts over a threshold length of about 40 repeats have the ability to form stable secondary structures such as hairpin loops, which can impede Okazaki fragment ligation and replication fork progression (Lahiri et al 2004). This likely contributes to the increased levels of replication fork stalling and slow fork progression detected in expanded repeats. Expanded CAG/CTG tracts show both instability, a propensity to change in length, and fragility, an increased tendency to break (Callahan et al 2003). Several

DNA repair mechanisms have been implicated in the prevention of CAG repeat fragility and instability, such as double-stranded break repair, nucleotide excision repair, and postreplication repair (PRR) (Sundararajan et al 2009)(Lahue & Slater 2003)(Daee et al 2006).

The gene *TRF4* was first discovered in a screen for mutations in *Saccharomyces cerevisiae* that were synthetically lethal with mutations in DNA topoisomerase I (Sadoff et al 1995). Δ*trf4* is defective in chromatin condensation, leading research groups to originally implicate it in chromatin structuring (Sadoff et al 1995). *TRF5*, the functional homolog of *TRF4*, was later discovered in a screen for genes whose overexpression diminished the synthetic lethality of *Δtrf4Δtop1* (Castano et al April 1996). The proteins coded by *TRF4* and *TRF5* are 57% identical and 72% similar. A double mutant of *Δtrf4Δtrf5* is inviable, suggesting that their functions overlap and serve an essential role for the organism (Castano et al April 1996). However, these two genes may additionally perform some separate functions due to differences in protein interactions and drug-sensitivity phenotypes (Edwards et al 2003). Trf4p is expressed at four times the level as trf5p, which may also explain phenotypical differences in the mutants (Reis and Campbell 2007). *TRF4* and *TRF5* constitute a novel gene family, which has been evolutionarily conserved, with homologues identified in *S. pombe, Drosophila,* and humans (Castano et al April 1996).

TRF4, along with its functional homolog, *TRF5*, codes for polymerase Polσ (Wang et al 2002), formerly named Polκ (Wang et al 2000). This polymerase is thought to be distantly related to the β-polymerase superfamily (Wang et al 2002). Early research found nucleotidyltransferase activity for *TRF4* (Wang et al 2000). Like DNA polymerase β, it showed a distributive mode of action, polymerizing one nucleotide at a time and dissociating after each

nucleotide (Uhlamann 2000). Polσ was the fourth essential nuclear polymerase identified in yeast (Carson and Christman 2001).

TRF4 Function in Repair

The hypersensitivity of *Δtrf4* to certain DNA-damaging agents has suggested a possible role for *TRF4* in DNA repair. First, *Δtrf4* mutants are hypersensitive to camptothecin (CPT), an antitumor agent that kills cells by initiating double stranded breaks in DNA (Walowsky et al 1999). Since defects in double-stranded break repair can cause hypersensitivity to CPT, this finding may implicate *TRF4* in double-stranded break repair (Walowsky et al 1999). Δ*trf4* mutants are also hypersensitive to MMS, which is an alkylating agent that causes DNA lesions similar to CPT (Walowsky et al 1999). This phenotype further points to some role of *TRF4* in double stranded break repair, particularly through homologous recombination (Walowsky et al 1999). In addition, *Δtrf4* is not hypersensitive to killing by UV irradiation, showing that the chromatin structure is not altered enough in the mutant for all repair to be disrupted (Walowsky et al 1999).

Finally, *Δtrf4*'s phenotype of hypersensitivity to MMS but not UV irraditation is also characteristic of base excision repair (BER) mutants (Gellon et al 2008). Recently, trf4p has been found to have dRP lyase activity, which suggests that trf4 may function as the homologue of mammalian Pol β in a BER pathway in yeast (Gellon et al 2008). In short patch base excision repair, a damaged base is removed by DNA glycosylase forming an AP site, which is cleaved by an AP endonuclease (Liu et al 2007). A polymerase with a dRP lyase function is needed to cleave the 5' deoxyribose phosphate that is left by the AP endonuclease, so that the polymerase can replace the removed base (Lui et al 2007). So far, only an alternative long-patch pathway for

BER has been discovered in yeast, but this recent discovery suggests that trf4 may function in a possible yeast short patch mechanism (Gellon et al 2007).

TRF4 Function in Cohesion

The double mutant of *Δtrf4Δtrf5* is lethal due its inability to complete S phase, while *TRF4/5* single mutants show S phase defects, leading to failure to establish sister chromatid cohesion (Wang et al 2000, Edwards et al 2003). This was demonstrated via a fluorescent tag on chromosome centromeres (Wang et al 2000, Edwards et al 2003. *TRF4* has also been implicated in the maintenance of cohesion throughout the cell cycle because it was found to be necessary to maintaining cohesion in metaphase-arrested cells (Uhlamann 2000). Sister chromatid cohesion is necessary to ensure that chromatids are together during mitosis to align at the metaphase plate, and the cohesin complex is broken-down during anaphase to allow the chromatids to segregate (Uhlamann 2000). The cohesin complex is composed of Smc1, Smc3, Scc1, and Scc3, and it is loaded onto chromosomes by Scc2-Scc4 at the cohesion attachment regions (CARs) (Uhlamann 2000). It is thought that cohesive bridges are established at the replication fork during S-phase, so that sister chromatids are never

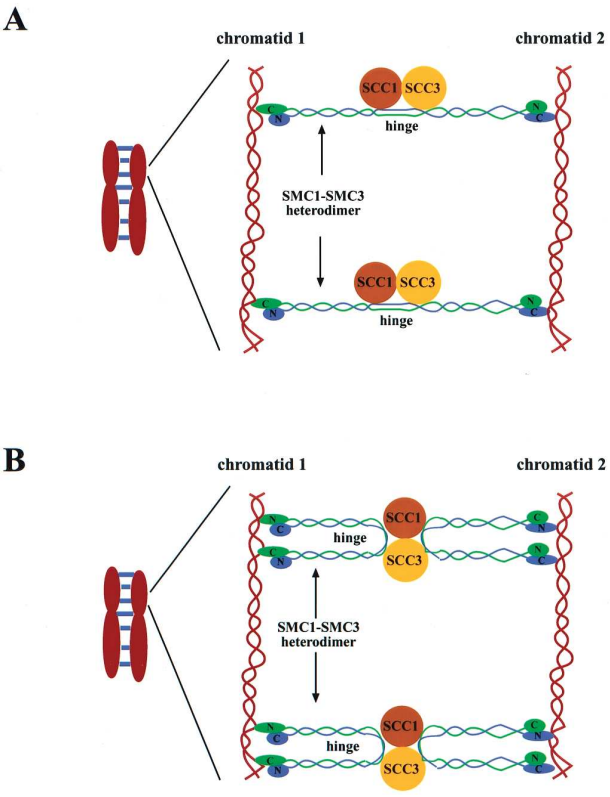

Figure 1. Potential Mechanisms for Sister Chromatid Cohesion. Above are two potential mechanisms for the cohesin complex. Although the structure of the cohesin complex is not known, it is known to be a significant barrier to the passage of the replication fork. (Carson and Christman 2001)

apart (Carson and Christman 2001). Since the cohesin complex is located at the CARs from G1 onward, it would provide a significant barrier to progressing replication forks, suggesting the need for coordination between replication and cohesion (Figure 1)(Carson and Christman 2001).

Since *TRF4* is necessary for sister chromatid cohesion and its possible involvement with replication through its DNA polymerase activity, trf4p/polσ was implicated as the possible link between the replication and cohesion machinery (Wang et al 2000). Trf4p/polσ physically associates with both Smc1, a member of the cohesin complex, and pol ε, a processive nuclear DNA polymerase thought to be involved in leading strand synthesis (Castano et al March 1996) (Edwards et al 2003). Finally, Trf4p is associated with the chromosome from late G1 until the metaphase-to-anaphase transition, further suggesting involvement with cohesion (Wang et al 2002). Proponents of this model suggest a polymerase-switching mechanism similar to the already established polymerase switch carried out during Okazaki fragment synthesis by the replication factor C clamp-loader complex (Figure 2) (Carson and Christman 2001). The Ctf18 alternative replication factor C-like complex (RFC) may promote a switch at the CARs from the processive polymerases polδ or polε to polσ, in order to allow the replication fork to bypass these regions (Hanna et al 2001). The Ctf18-RFC includes Ctf18, Dcc1, Ctf8, RFCp40, RFCp38, RFCp37, and RFCp36 (Bermudez et al 2003). It is essential for sister chromosome cohesion and is able to both load and unload PCNA onto DNA (14).

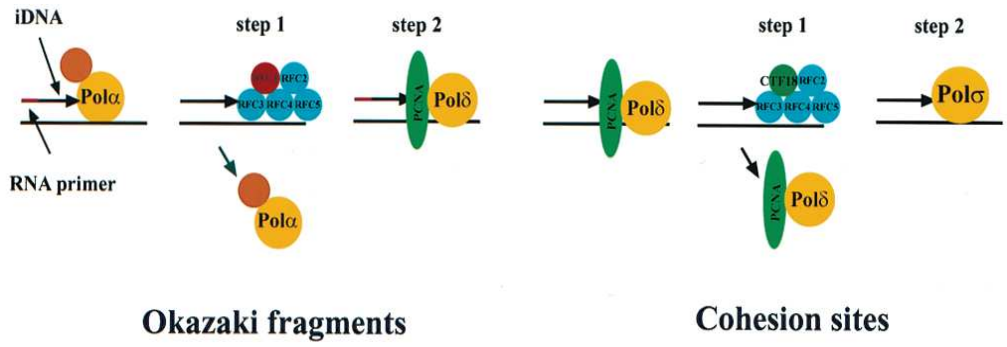

Figure 2. Potential Polymerase Switching Mechanism. This figure compares the potential polymerase switching mechanism of Polσ at CARs to the known polymerase switching mechanism at Okazaki fragments. (Carson and Christman 2001)

The possible involvement of *TRF4* in cohesion can explain the mutant's chromatin condensation defects because the binding of cohesin at the CARs can affect chromatin structure (Uhlamann 2000). *TRF4*'s potential role in replication may also explain the synthetic lethality of *Δtrf4Δtop1*, since *TOP1* is the primary swivel that maintains appropriate DNA topology for replication, and *TRF4* may also be a key replication factor involved in DNA structure through cohesion (Wang et al 2000). Finally, since cohesion defects can cause hypersensitivity to DNA damage, it is unknown whether *Δtrf4*'s hypersensitivity phenotypes can be attributed to cohesion effects or an actual DNA repair function for *TRF4* (Uhlamann 2000).

Despite this evidence, the role of *TRF4*/polσ in cohesion remains controversial. First of all, some have disputed the finding that Trf4p has any DNA polymerase function (Saitoh et al 2002). The recent discovery of a poly-A RNA polymerase function for *TRF4* has implicated this gene in the degradation of aberrant RNAs (see below). Some have argued that the cohesion defects in *Δtrf4* mutants are caused indirectly by changes in the expression of cohesion-related proteins due to defective RNA surveillance mechanisms (Bermudez et al 2003). Additionally, instead of a polymerase switching mechanism, the switch occurring at the CARs may be of the replicative RFC for the RFC-Ctf18, with no involvement of polσ (Bermudez et al 2003). One

study contradicted previous results by finding only a very minor effect of deleting *TRF4* on sister chromosome cohesion and chromosome segregation (Petronczki et al 2004). These authors argue that if *TRF4* is actually essential for cohesion to occur its deletion would have the same phenotype as RFC-Ctf18 subunit deletions (Petronczki et al 2004). However, they do acknowledge that the defect phenotype may be decreased because of *TRF4*'s redundancy with *TRF5*. It remains unknown whether *TRF4*'s function lies primarily on an RNA or DNA level in yeast.

TRF4 Function in RNA Degradation

The recent finding that Trf4p and Trf5p exhibit poly(A) polymerase activity (Kadaba et al 2004) has revolutionized the type of research being done on *TRF4*. Previous to this finding, studies reported Pol(A) polymerase activity for Cid13, Trf4's homologue in fission yeast (Saitoh et al 2002). This activity seemed to be promoting the degradation of unstable pre-tRNAs in a mechanism similar to one already detailed in *E. coli* (Kadaba et al 2004). Though Cid13's effect initially led researchers to speculate that it might not actually be a homologue of Trf4, research soon began to suggest that Trf4 also plays a role in RNA metabolism (Saitoh et al 2002).

Before the discovery of Trf4's role on an RNA level, there were two general pathways for mRNA degradation in yeast (Kadaba et al 2004). The first was to shorten the mRNA's poly(A) tail, which generally confers stability in the cytoplasm, followed by 5' cap removal and body degradation by Xrn1p (Kadaba et al 2004). Alternatively, the mRNA could be deadenylated then degraded by the exosome which is a complex of 3' to 5' exonucleases (Kadaba et al 2004, Egecioglu et at 2006). A new role for Trf4 has been discovered in the degradation of aberrant mRNAs. This degradation pathway functions differently than the two

original pathways because it occurs in the nucleus and targets certain mRNAs for degradation by adding a poly(A) tail rather than degrading it (Neil et al 2009).

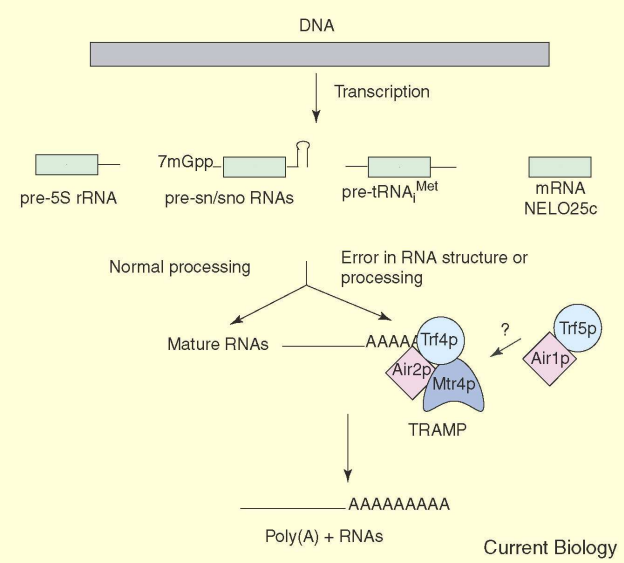

Figure 3. TRAMP Complex Model. This figure shows the TRAMP complex functioning in the degradation of nonfunctional pre-5S rRNA, sn/snoRNA, pre-tRNA, and mRNA. (Anderson 2005)

Trf4p is the second poly(A) polymerase (PAP) isolated in yeast (Anderson 2005). In contrast to *TRF4*'s role, the canonical PAP, Pap1, functions to stabilize mRNAs and enhance translation (Anderson 2005). Much is still not understood about the differences between the stabilizing poly(A) tails from Pap1 and the tails created by Trf4, which target mRNAs for degradation. One model is that poly(A) binding protein (Pab1p) may bind to the poly(A) tails of mRNAs that are destined for the cytoplasm, protecting them from degradation, while the poly(A) tails synthesized by Trf4 do not bind Pab1p (Libri 2010). The size of the poly(A) tail may also be important, as shorter tails are thought to signal the exosome (Libri 2010).

Trf4p is contributing to the degradation of mRNA, among other types of RNA, by working as the catalytic subunit of the TRAMP complex (Figure 3)(Anderson 2005). The TRAMP4 complex contains Trf4p, Air2p, and Mtr4p, while the TRAMP5 complex consists of Trf5p, Air1p, and Mtr4p (Houseley & Tollervey 2008). Air1p and Air2p provide the RNA-binding activity of TRAMP while Mtr4 is a helicase that is thought to connect the exosome to the complex (Houseley & Tollervey 2008). TRAMP4 and TRAMP5 seem to target at least

partially different substrates for degradation (Houseley & Tollervey 2008), and one study found trf5p to be more localized to the nucleolus, while Trf4p was spread throughout the nucleus (Anderson 2005). However, polyadenylation of some TRAMP4 substrates is also reduced when *TRF5* is deleted, though to a lower extent, which suggests that they may act on some similar substrates, or Trf5p affects Trf4p function in some other way (Egecioglu et al 2006).

In addition to mRNA, the TRAMP4/5 complex has been observed to target various non-coding RNAs for degradation by the exosome, including tRNAs, pre-rRNAs, and rRNAs (Anderson 2005). These targets are not functional in the cell, often mutated or incorrectly processed (Egecioglu et al 2006). This surveillance pathway also targets processing and degradation intermediates of small nuclear RNAs (snRNAs), which are involved in pre-mRNA splicing, and small nucleolar RNAs (snoRNAs), which are involved in rRNA processing. (Egecioglu et al 2006)(Allmang et al 1999). Many substrates that TRAMP targets are ribonucleoprotein complexes, and TRAMP is likely signaled when surveillance mechanisms notice changes in the speed of assembly or these complexes or misfolding (Houseley & Tollervey 2008).

Another target of TRAMP is cryptic non-protein coding RNAs (ncRNAs), which are kept at very low concentrations in wild-type yeast (Houseley & Tollervey 2008). One type of ncRNA is cryptic unstable transcripts (CUTs), which are immediately degraded following transcription (Houseley et al 2007). CUTs are transcribed by RNA pol II and have both a 5' cap and 3' poly(A) tail, but they are not protein-coding (Housely et al 2007). Little is known about their potential function in the cell, but they may play a role in establishing silenced chromatin regions (Houseley et al 2007). Though early research into these transcripts suggested that they may come from unspecific transcriptional noise, more recent research has found that they usually come

from divergent transcription at bidirectional promoters (Neil et al 2009). Since many CUTs overlap promoters and the 5' untranslated regions of mRNAs, their presence could interfere with gene expression (Neil et al 2009).

After the discovery of this novel role of trf4p in RNA surveillance, some researchers claim that Trf4p functions solely as a poly(A) polymerase, though the protein's role as a DNA polymerase is still debated (Haracska et al 2005). One study found that *Δtrf4* mutants have elevated levels of histone mRNA, implicating TRAMP4 is a possible negative regulator of histone levels (Reis & Campbell 2007). This study also notes that excess histones in Δ*trf4* could also explain the mutant's sensitivity to DNA-damaging agents and chromatin structure defects (Reis & Campbell 2007). However, the researchers were unable to detect polyadenylation by trf4p on these histone mRNAs, suggesting that trf4p may still have some sort of role independent of its poly(A)-polymerase role in the TRAMP complex. Other researchers studying *TRF4*'s role in TRAMP believe that TRAMP and the exosome may play a role in DNA damage repair, independent of TRAMP's role in RNA surveillance (Houseley et al 2007). Further research is needed to elucidate exactly what role trf4p is playing in yeast.

TRF4 Role in Repeat Maintenance

No previous research has been done exploring a possible role for *TRF4* in the maintenance of trinucleotide repeats. Since several repair pathways have been implicated in CAG repeat fragility and instability, and *TRF4* has a potential role in repair, we were interested in whether this gene could affect CAG repeat maintenance. Additionally, *TRF4*'s role in RNA regulation is of interest because RNA:DNA hybrids at the replication fork, called R loops, have been shown to contribute to genetic instability, potentially through replication fork stalling (Mirkin & Mirkin 2007) (Huertas & Augilera 2003). My research in *Saccharomyces cerevisiae*

suggests a role for *TRF4* in preventing yeast CAG repeat fragility and instability. This paper will explore what this role may be, with an overall goal of further elucidating the function of *TRF4* in the yeast genome as a whole.

Methods

Creating Mutant Strains

A Δ*trf4*::KAN mutant was created using the Stanford deletion set of BY4705 haploid yeast cultures, selecting the knock-out strain of *TRF4* disrupted by a KanMX marker, which confers resistance to G418. The disrupted *TRF4* region was isolated by PCR with 18-20 base-pair (bp) long primers, which were complementary to the regions 60-100 bp upstream and downstream of the gene and at least 50% guanine and cytosine (Figure 1). The PCR reaction protocol called for 50µl δH_2O, 20µl 5X buffer (w/o $MgCl_2$), 6µl 25mM $MgCl_2$, 10µl 10pmol/λ of the forward primer, 10µl 10pmol/λ of the reverse primer, 2µl 10mM dNTPs, 2µl DNA polymerase, and a small section of the yeast colony. Gel electrophoresis was used to verify that this PCR in fact isolated the DNA fragment of expected size.

Next, the amplified Δ*trf4* region disrupted with KanMX was transformed into BY4705 wild-type yeast strains containing a Yeast Artificial Chromosome (YAC). The two YACs contained either no CAG repeats or 70 CAG repeats, as well a LEU2 and a URA3 marker. An acetate lithium procedure was used to transform the PCR product into *S. cerevisiae*. Transformation products were plated on G418 plates, in order to select for yeast that now had *TRF4* disrupted by KanMX.

Potential transformants were patched onto Ura^-Leu^- plates to select for strains containing the YAC. PCR was used to verify in which strains *TRF4* had been disrupted. The protocol called

for 6.25 µl δH_2O, 2.5 µl 5X buffer (w/o $MgCl_2$), 0.75 µl 25mM $MgCl_2$, 1.25 µl 10pmol of the forward primer, 1.25 µl 10pmol of the reverse primer, 0.25 µl 10mM dNTPs, 0.25 µl DNA polymerase, and a small section of the yeast patch. A 5' primer about 300 bp upstream of the gene and the 3' KanB primer, complementary to a sequence within the KanMX marker, were used (Figure 1). Running these PCR products on a gel allowed the transformants to be identified as the strains exhibiting a band of the desired size.

Due to the instability of the repeat tract, the transformants were tested to determine if their tract lengths were in fact 70 repeats. These colonies underwent PCR with primers flanking the CAG repeat region on the YAC. The protocol was modified because normal PCR reactions have difficulty replicating through regions of CAG repeats. It called for 5.8µl δH_2O, 1.25µl 10X buffer (w/o $MgCl_2$), 1.25µl 2mM $MgCl_2$, 2.5µl GC-rich buffer, 0.625µl 10pmol of the forward primer, 0.625µl 10pmol of the reverse primer, 0.25µl 10mM dNTPs, 0.2µl Phoenix Polymerase, and a small section of the colony being tested. Products were run on 2% Metaphor agarose gel in order to determine tract length by the band migration. Strains were stored in glycerol stock at -70ºC.

The same procedure was carried out in order to make the Δ*trf5* mutant strain, except with primers specific to this gene's region.

In order to create a Δ*trf4*Δ*rad52* double mutant, a Δ*rad52*::HIS3 mutant strain developed by another lab member, Ranjith Anad, was obtained. The same PCR method was used to isolate the HIS3 disrupted region using primers flanking the *RAD52* region. This PCR product was transformed by the same method into the Δ*trf4*::KAN CAG-0 and *trf4*::KAN CAG-70 strains. The same method as above was used to verify the desired strains.

To ease the creation of further double-mutants, Δ*trf4*::HIS3 strains were created in CAG-0 and CAG-70 backgrounds. To create these strains, PCR was performed on a plasmid containing the HIS3 marker with primers flanking the HIS3 sequence, which also had homology to the sequences upstream and downstream of the *TRF4* gene. This PCR product was transformed into the Δ*trf4*::KAN strains containing the no-repeat YAC and the 70 repeat YAC. Transformation products were plated onto $His^{-}Ura^{-}Leu^{-}$ plates to select for the HIS3 marker disrupting *TRF4* as well as the YAC. The same PCR protocol was used to verify the transformants, except that a 3' HIS primer, which was complementary to a sequence within the HIS3 marker, was used instead of the 3' KanB primer.

Next, in order to create the Δ*trf4*Δ*ctf18* double mutant, Δ*ctf18*::KanMX strains containing the no-repeat YAC and CAG-70 YAC were obtained from another lab member, Lionel Gellon. PCR was performed on the Δ*trf4*::HIS3 strain to isolate the disrupted *TRF4* region, and this product was transformed into the Δ*ctf18*::KanMX strains to create the double mutant strains.

Finally, Δ*trf4*Δ*rad5*, Δ*trf4*Δ*rad6*, and Δ*trf4*Δ*rad30* mutant strains containing the YACs were created. The *RAD5*, *RAD6*, and *RAD30* regions disrupted by KanMX were isolated using PCR from the Stanford deletion set and transformed into Δ*trf4*::HIS3 strains. Δ*Rad6* and Δ*rad30* strains containing the CAG-0 and CAG-70 YACs were also created using the same method used to obtain the original Δ*trf4*::KanMX strain.

Fragility and Instability Assays

The disrupted strains with the correct tract lengths were used in the fluctuation analysis assay (Figure 4). For each assay a single mutant strain was used, and assays were performed for both the mutants with no CAG tract and those with a CAG-70 tract. Cells from one mutant

colony were suspended in 10 tubes of YC-leu media, and incubated to grow for 7 cycles. 100µl from each tube was plated on a FOA-leu plate. This selected for FOA resistance, which indicates a breakage event in the repeat tract. 100µl of each of the 10 tubes was combined, and 100µl of a 10^{-4} dilution of this solution was plated on two YC-leu plates, in order to determine the total cell count. The rate of FOA-resistance was determined using the method of maximum likelihood with the data for the number of colonies growing on the FOA-leu plates and the total cell count. The rate was defined as the likelihood that a mutation will occur per cell per generation. Three fragility assays were carried out for each mutant, with the average rate of FOA-resistance for these three assays was used to represent the breakage rate in the repeat tract.

The instability assay was performed on each mutant in order to assess instability of the CAG repeat tracts (Figure 4). The tract lengths of colonies on the CAG(70) YC-leu plate from the fragility assay were determined via PCR. PCR products that corresponded to tract lengths larger than 70 repeats were considered expanded, while tract lengths smaller than 70 repeats were contracted. Calculations were performed to determine the percent of colonies that had expanded and contracted repeat tracts.

Figure 4. Fragility and Instability Assays.

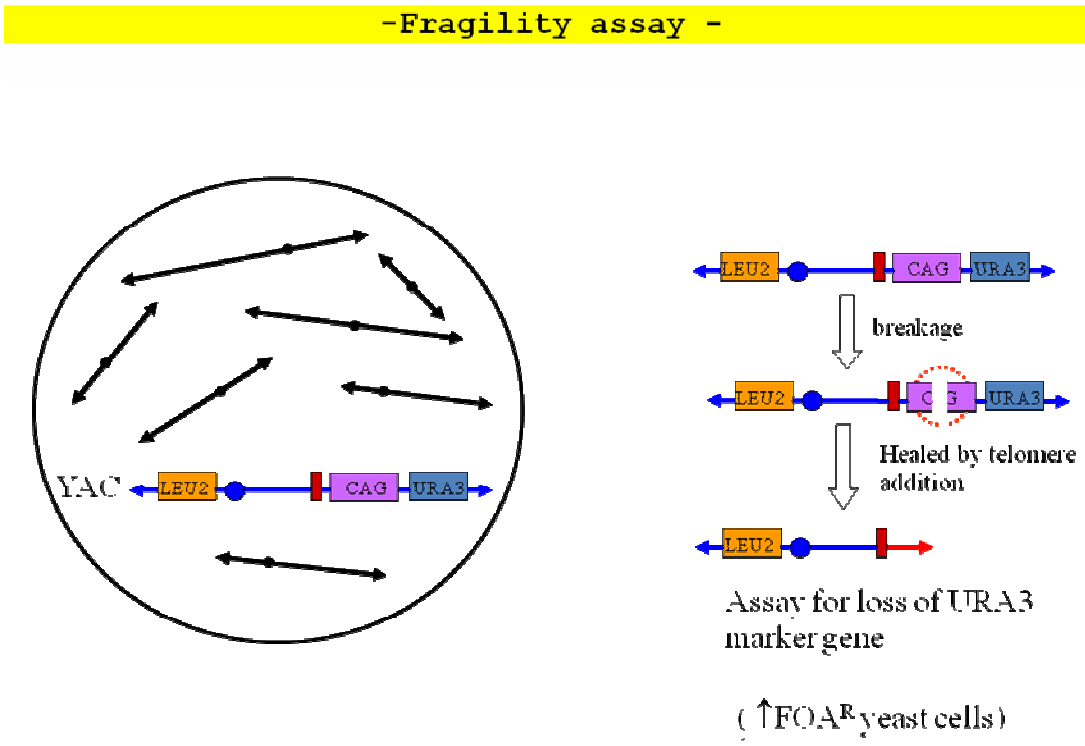

RNaseH Experiment

In order to explore the potential contribution of *TRF4*'s RNA-level role in the Δ*trf4* fragility and instability phenotypes, we designed an experiment to determine the effect of potential RNA:DNA hybrids. We requested two plasmids from the Koshland laboratory in Berkley, CA, one containing the RNaseH1 gene and one control plasmid without this gene. In order for the RNaseH1 plasmid to be created by the Koshland lab, the RNaseH1 gene was isolated by PCR from the NIH 3T3 cDNA library and cloned into the multiple cloning site of the p425 Funk vector (Figure 5) with EcoRI. Since this site follows a GPD promoter, this gene is expressed constitutively. The control plasmid was the p425 Funk vector without the RNaseH1 gene inserted.

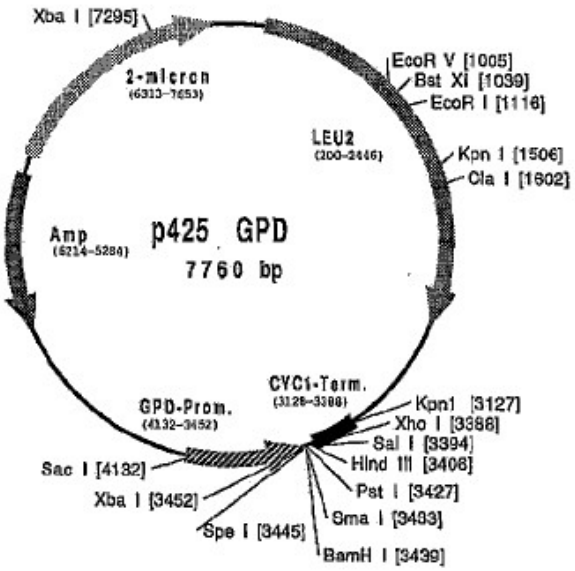

Figure 5. p425 Leu2 Funk vector.

In order to amplify these two plasmids for use in our experiment, the plasmids were first transformed into bacterial competent cells, according to a standard heat shock procedure. After, these new bacteria strains replicated, the Zyppy Plasmid miniprep was carried out to isolate the plasmids from the bacteria. Restriction enzyme digests were performed to check the plasmids, and these digests were run on 0.8% agarose gels. A SacI digestion was performed on the two plasmids using 5µl of plasmid, 2µl NEBuffer 4, 2µl BSA 10x, 1µl SacI, and 10µl water. This mixture was incubated at 37º for 1 hour. Next, the two

plasmids from the transformation were digested for one hour at 37º with EcoRI. Reactions contained 5µl of plasmid, 2µl NEBuffer EcoRI, 1µl EcoRI, and 12µl water. These digestions showed that neither of the plasmids sent to us actually contained the RNaseH gene, and they are likely both control plasmids. This realization is described in more detail in the results section. We had meanwhile begun the experiment using these plasmids, and we decided to continue with the control experiment while we waited to obtain or create a plasmid containing RnaseH1.

Since the marker for the plasmid is the LEU2 gene and our YAC also contains LEU2, we switched out the LEU2 marker for a TRP1 marker. A separate plasmid containing TRP1 was obtained and primers were designed that flanked the TRP1 sequence and also had homology to the sequences flanking the LEU2 marker in the Funk vector. PCR was carried out using these primers and the TRP1 plasmid in order to isolate the TRP1 sequence. This PCR product was then transformed simultaneously with the control vector into wild-type BY4705 yeast and the Δ*trf4* mutants containing the YAC with 70 repeats (with the intention to do a later transformation using strains with the no repeat YAC). The transformation products were plated on -trp-ura plates to select for strains that contained plasmids with the TRP1 marker and the YAC, which contains a URA3 marker. This created wild-type and Δ*trf4* strains containing plasmids equivalent to the p424 Funk vector (Figure 6).

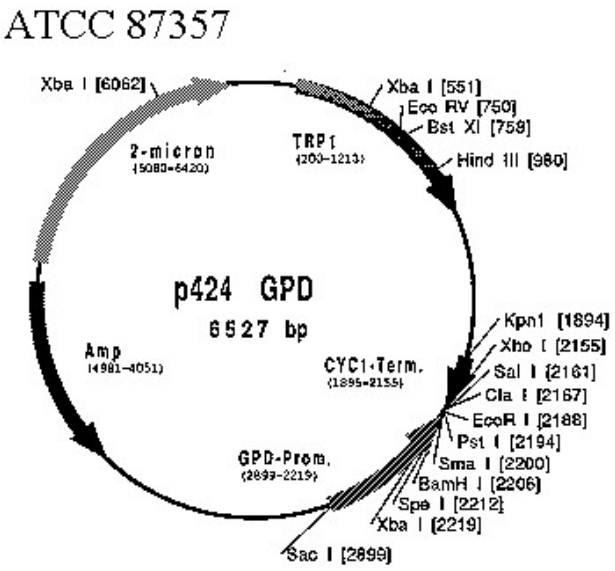

Figure 6. p424 Trp1 Funk Vector

Next, the plasmids were isolated from four yeast strains in both the wild-type and Δ*trf4* backgrounds (Hoffman & Winston, 1987). Since the plasmid isolation efficiency from yeast is low, these plasmids were then transformed into bacteria and isolated with a miniprep, using the same procedure used with the original plasmids. A Cla1 restriction digest was performed on these plasmids for one hour at 37º. The digests contained 5µl of plasmid, 2µl NEBuffer 1, 2µl BSA 10x, 1µl Cla1, and 10µl water.

Results

Δ*trf4*, Δ*trf5,* Δ*trf4*Δ*ctf18*, Δ*trf4*Δ*rad5,* Δ*trf4*Δ*rad52,* Δ*rad6,* Δ*trf4*Δ*rad6,* Δ*rad30*, and Δ*trf4*Δ*rad30* mutants were created in BY4705 budding yeast. In order to asses the effect of these genes on instability and fragility of CAG repeats, these knockouts were created in yeast strains containing a Yeast Artificial Chromosome (YAC). This YAC contained either no repeat tract or 70 CAG repeats. Fragility and instability assays were performed on these mutant strains.

Wild-type fragility and instability phenotypes

Prior research in our lab showed that wild-type yeast strains containing our YAC have an average rate of FOA resistance of $2.65*10^{-6}$ (SEM= 0.68) when no repeat tract is present and an average rate of $7.61*10^{-6}$ (SEM= 0.56) for a 70 repeat tract (Figure 7) (Priya Sundararajan). The rate of FOA resistance in our assay has been shown to be correlated to the rate of YAC breakage. Therefore, fragility has been shown to increase in the presence of CAG repeats in our system. Prior instability data showed that in wild-type yeast containing a 70 repeat YAC, 5.8% of colonies display a contraction in tract length, while 0.8% of colonies expand in tract length (Figure 8) (Priya Sundararajan).

Mutants for *TRF4* display increased CAG repeat fragility and instability, while deleting *TRF5* shows no effect

In order to determine if the gene *TRF4* has any effect on repeat fragility, fragility assays were performed on *Δtrf4* mutant strains. Three fragility assays were performed for the Δ*trf4* mutant with no repeat tract. For the CAG-70 strains, three assays were performed with the *TRF4*::HIS mutant, and one was performed for the *TRF4*::KAN mutant. The average breakage rate for Δ*trf4* was $3.61*10^{-6}$ (SEM=0.75) when there is no repeat tract and $63.45*10^{-6}$ (SEM=8.69) for CAG-70 strains (Figure 7). There was no significant increase in fragility over the wild-type for the mutants containing no repeats (pooled variance t-test, t=0.537, df=4.0, p=0.620). However, there was a significant increase in fragility for the CAG-70 tract in the Δ*trf4* mutant (pooled variance t-test, t=5.316, df=5, p=0.003).

Since *TRF5* is the redundant homologue of *TRF4*, we wanted to determine whether this gene might also increase fragility in CAG repeat tracts. Three fragility assays were performed for Δ*trf5* mutants containing the YAC with no repeats and mutants containing a 70 repeat tract (Figure 7). The average breakage rate for Δ*trf5* with no repeats was $4.77*10^{-6}$ (SEM=0.29), and the average breakage rate for Δ*trf5* CAG-70 was $12.38*10^{-6}$ (SEM=1.76). There was no significant increase in fragility over the wild-type for Δ*trf5* mutants with no repeats (pooled variance t-test, t=2.310, df=4, p=0.082). Additionally, there was no significant increase in fragility over the wild-type for mutants with 70 repeats (pooled variance t-test, t=1.678, df=4, p=0.169).

To explore if *TRF4* or *TRF5* plays a role in CAG repeat instability, instability assays were carried out in Δ*trf4* and Δ*trf5* strains (Figure 8). In the Δ*trf4* CAG-70 mutant, 15.4% of colonies displayed contracted repeat tracts, which is a 2.7 fold significant increase over the wild-

type (Fisher's exact test, p=0.0039). 3.08% of colonies were expanded, which is 3.9 fold increase over the wild-type phenotype, though not a significant increase (p=0.189). For the Δ*trf5* CAG-70 mutants, 5.2% of colonies were contracted and 2.6% of colonies were expanded. This represents a 1.1 fold decrease and a 3.3 fold increase over the wild-type phenotype, respectively (p=1, 0.245).

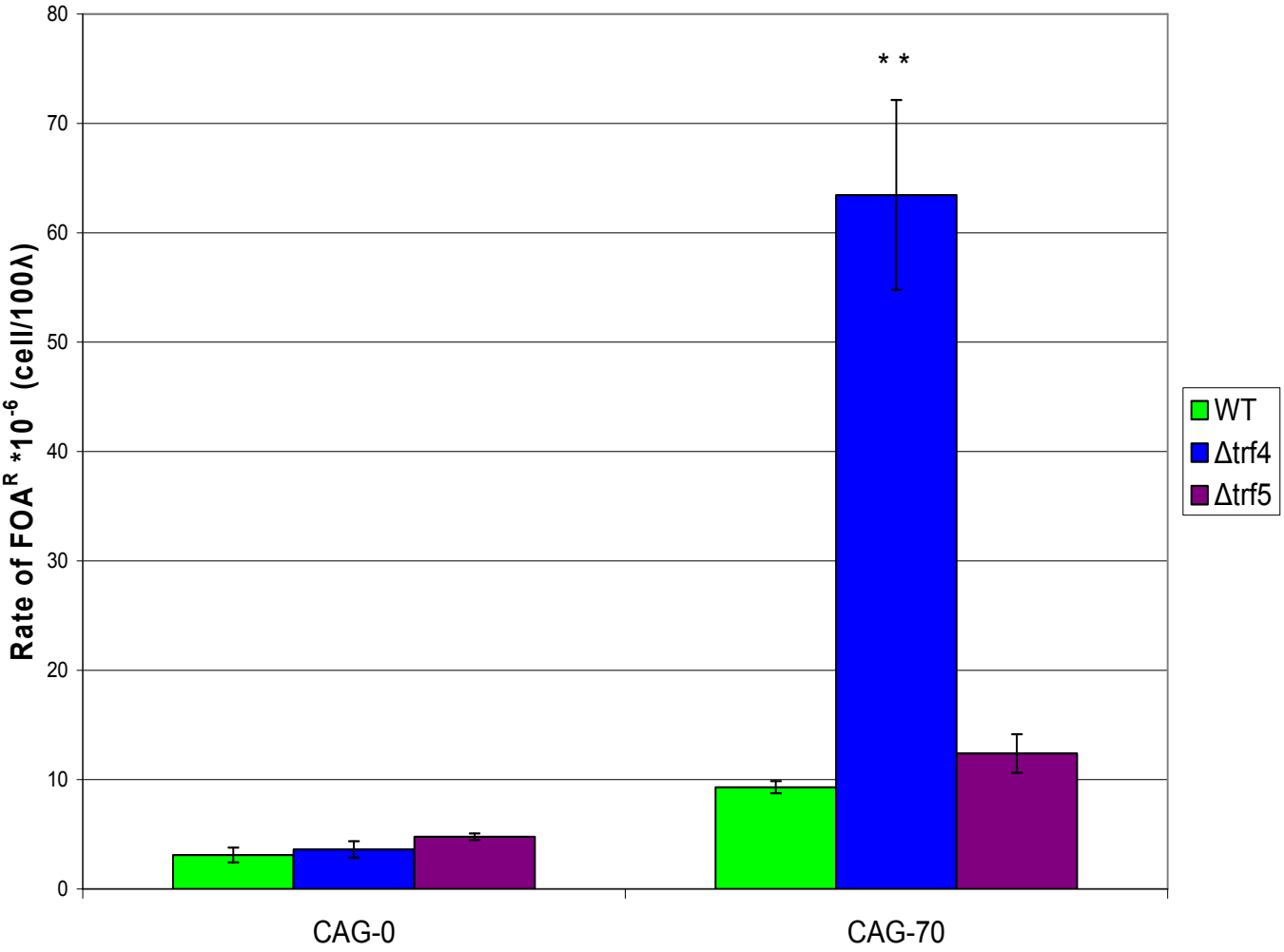

Figure 7. Δ*trf4* and Δ*trf5* Fragility Data Compared to Wild-Type Yeast. Error bars represent the standard error of the mean (SEM). The (*) symbol indicates p<0.05 compared to the wild-type, and (**) indicates p<0.01 (pooled variance t-test).

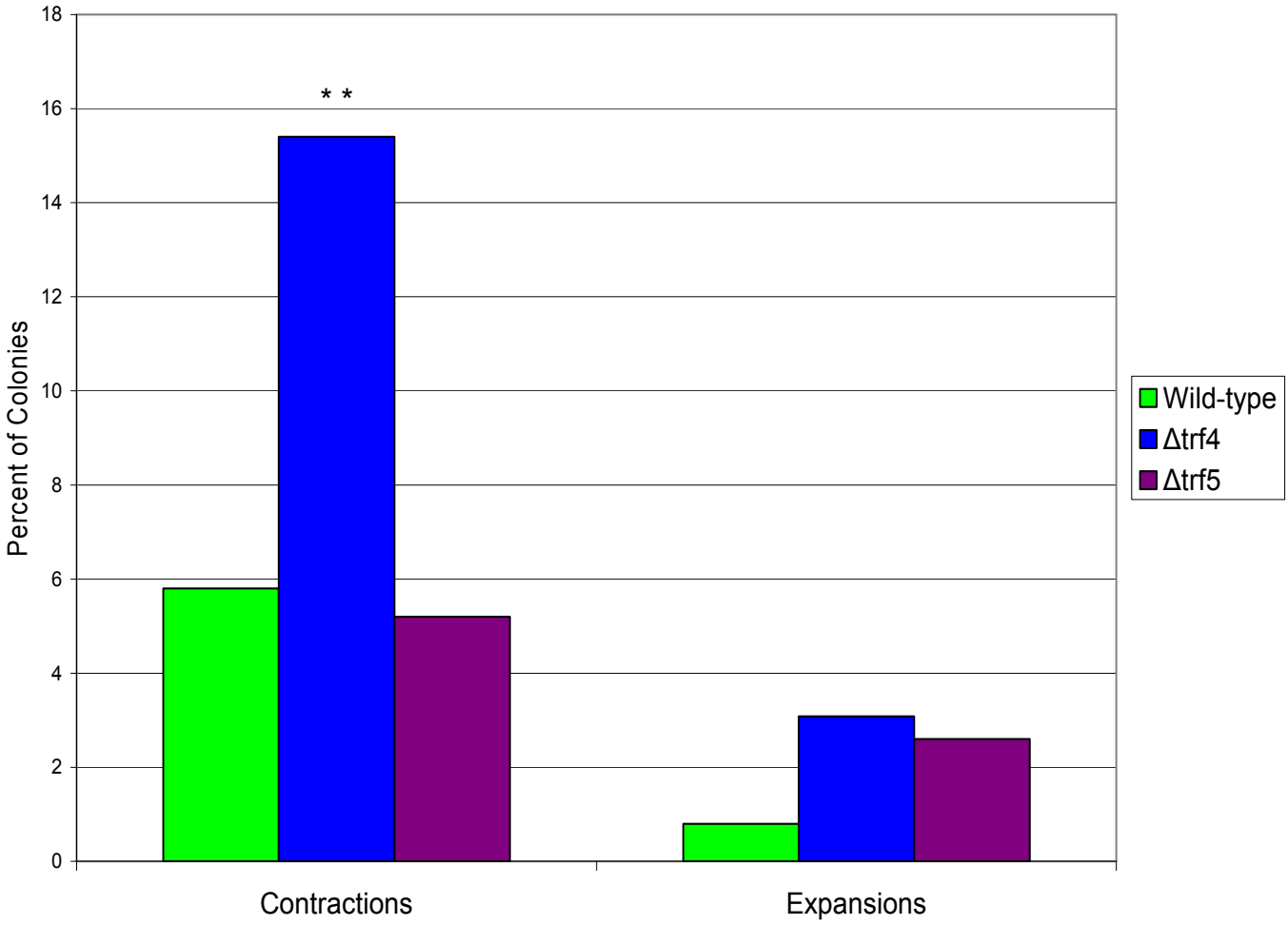

Figure 8. Δ*trf4* and Δ*trf5* Instability Data Compared to the Wild-type. The * symbol indicates $p<0.05$ in comparison to the wild-type, and ** indicates $p<0.01$ (Fischer's Exact Test).

Exploring a potential role for *TRF4* in double-stranded break repair

The gene *RAD52* is a member of the *RAD52* epistasis group, which functions in double-stranded break repair (Symington 2002). Rad52 is thought to target Rad51 to single stranded DNA, mediating strand invasion (Symington 2002). The doubled-strained break repair pathway has been shown to function in the prevention of both fragility and instability in CAG repeats (Sundararajan 2009). In order to determine whether the Δ*trf4* phenotype can be attributed to *TRF4* working in this pathway, a Δ*trf4*Δ*rad52* double mutant was created.

Δ*Rad52* mutants with no repeat tract have an average fragility rate of $5.3*10^{-6}$ (SEM=0.6), and mutants with 70 repeats have a rate of $24.35*10^{-6}$ (SEM=1.3) (Ranjith Anand). While the no repeat tract phenotype is not significantly different than wild-type (p=0.182), the 70 repeat phenotype is significantly increased from the wild-type (0.002). The Δ*trf4*Δ*rad52* double mutant with no repeat tract has a fragility rate of $4.1*10^{-6}$ (SEM=1.82). For the no repeat strains, the fragility rates for the wild-type, Δ*trf4*, Δ*rad52,* and Δ*trf4*Δ*rad52* are not significantly different (ANOVA, df=3,8, F=0.346, p=0.793). The Δ*trf4*Δ*rad52* double mutant with the 70 repeat tract has an average breakage rate of $121.18*10^{-6}$ (SEM=24.94). Statistical analysis shows that the 70 repeat strain fragility rate is significantly different among the wild-type, Δ*trf4*, Δ*rad52*, and Δ*trf4*Δ*rad52* strains (ANOVA, F=15.176, df=3,9, p=0.001). The double mutant's fragility rate is significantly higher than the wild-type (Bonferroni, α*=0.0167, p=0.00017), the Δ*trf4* single mutant (p=0.0088), and the Δ*rad52* single mutant (p=0.00033). (Figure 9)

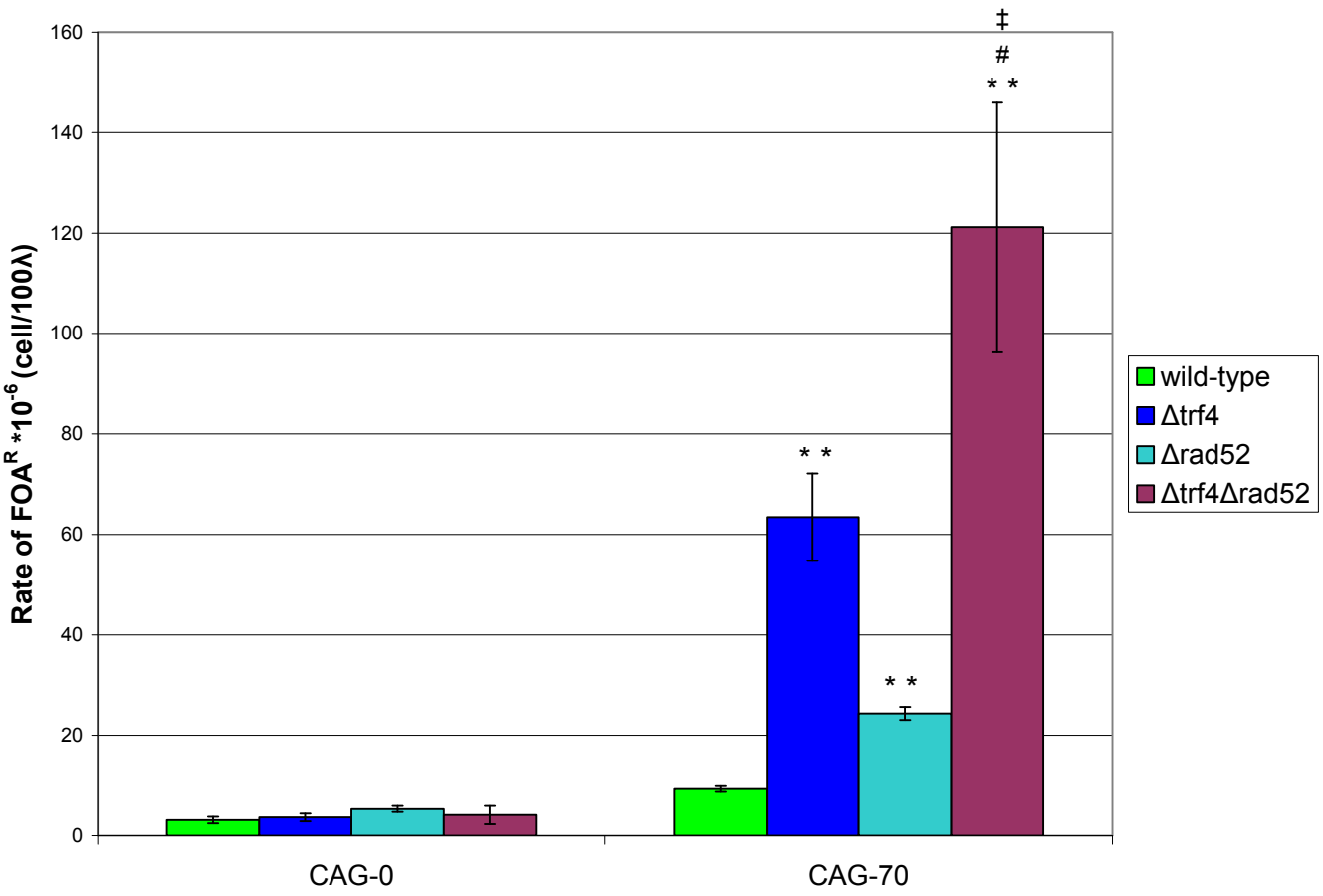

Figure 9. Δ*trf4*Δ*rad52* Fragility Data Compared to Wild-type, Δ*trf4*, and Δ*rad52*. Error bars represent the standard error of the mean (SEM). The * symbol indicates $p<0.05$ compared to the wild-type, and ** indicates $p<0.01$ (pooled variance t-test). ‡ denotes a significant difference from Δ*trf4*, while # denotes a significant difference from Δ*rad52* (Bonferroni multiple comparisons test, $p<\alpha^*$).

Δ*Rad52* instability was assayed by Priya Sundararajan. This mutant showed 10.7% contractions, which was a 1.8 increase over the wild-type, though not statistically significant (p=0.107). Δ*Rad52* also showed 1.4% expansions, which was a 1.8 fold increase over the wild-type and also not significant (p=0.307). The Δ*trf4*Δ*rad52* double mutant displayed 17.3% contractions, which is a significant 3 fold increase over the wild-type (p=0.0018). However, this phenotype is not significantly different than the Δ*rad52* or Δ*trf4* phenotypes (p=0.185, 0.724). The double mutant also displayed 2.9% expansions. This was not a significant difference over the wild-type (p=0.16), Δ*trf4* (p=1), or Δ*rad52* (p=0.65). (Figure 10)

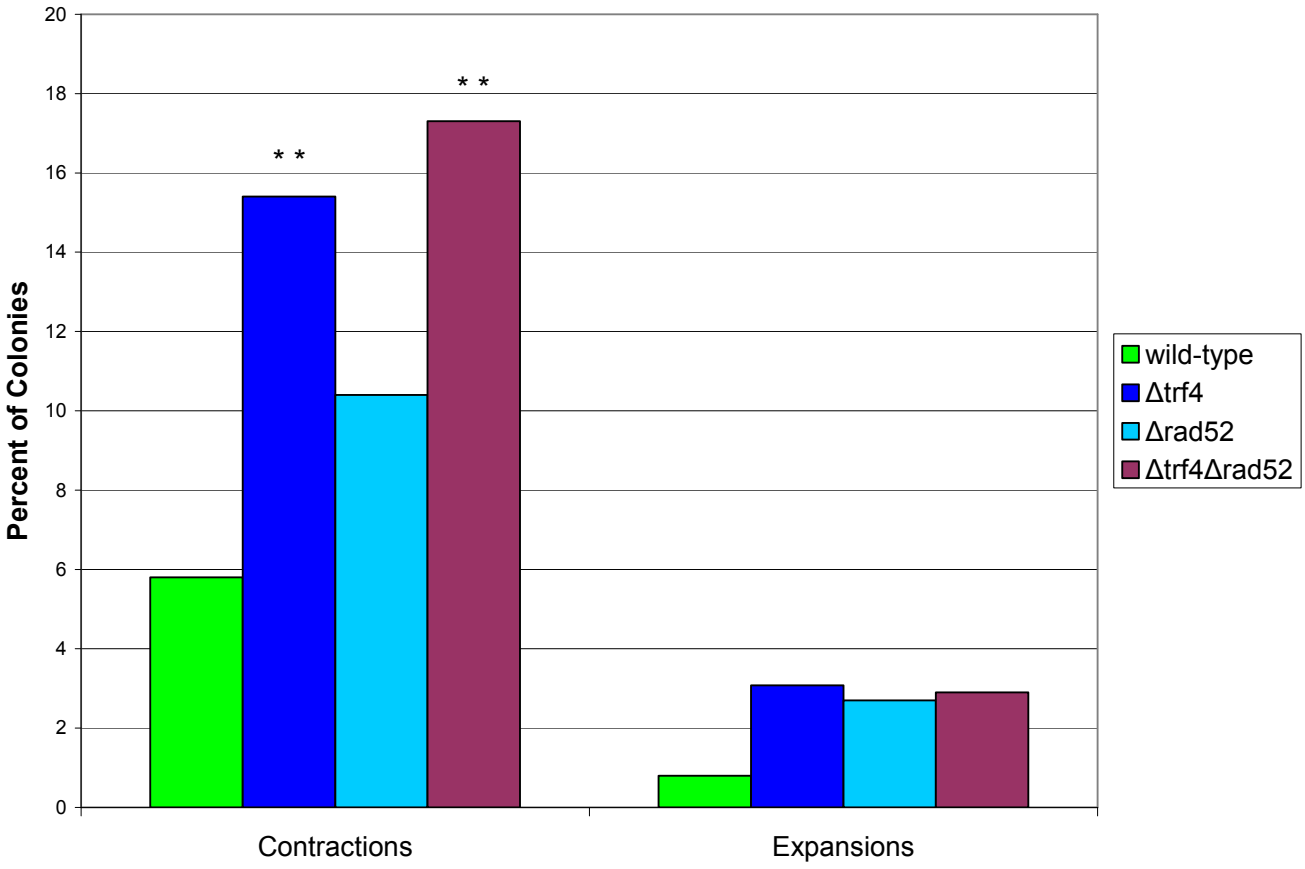

Figure 10. Δ*trf4*Δ*rad52* Instability Data Compared to the Wild-type, Δ*trf4,* and Δ*rad52*. The * symbol indicates p<0.05 in comparison to the wild-type, and ** indicates p<0.01 (Fischer's Exact Test). ‡ denotes a significant difference from Δ*trf4,* while # denotes a significant difference from Δ*rad52* (Fischer's Exact Test).

Examining *TRF4*'s potential involvement with the Ctf18-RFC

Ctf18 is a component of the alternative clamp loader/ unloader complex, RFC-Ctf18. Since mutants for the components of this complex show cohesion defects, it has been implicated in sister chromatid cohesion. An experiment with Δ*trf4*Δ*ctf18* was originally planned to test *TRF4*'s potential role in sister chromatid cohesion, and whether this role is contributing to its mutant's fragility and instability phenotypes. However, though concurrent research found increased CAG repeat fragility and instability in *CTF18* mutants, mutants for genes involved in sister chromatid cohesion, *CHL1, SCC1-73,* and *SCC2-4,* all showed no increased fragility or instability phenotype over the wild-type (Lionel Gellon, unpublished data). This indicates that *CTF18* is stabilizing CAG repeats in a mechanism that is likely cohesion-independent. The complex's ability to load and unload PCNA onto single-stranded DNA may contribute to a replication fork stabilization function, potentially by minimizing secondary structure formation. Thus, although the Δ*trf4*Δ*ctf18* experiment does not necessarily serve its original purpose to explore *TRF4*'s cohesion role, it examines whether *TRF4* may be affecting repeat fragility and instability in the same pathway as *CTF18*.

Three fragility assays were performed in the Δ*trf4*Δ*ctf18* mutant background for both the no repeat tract and CAG-70 repeat strains (Figure 11). Research conducted by Lionel Gellon determined that the average breakage rate for Δ*ctf18* mutants with no repeats is $6.1*10^{-6}$ (SEM=0.68), which represents a significant increase over the wild-type (pooled variance t-test, t=3.188, df=4, p=0.033). The average breakage rate for Δ*ctf18* CAG-70 mutants is $40.3*10^{-6}$ (SEM=10.17), which is also a significant increase over the wild-type (pooled variance t-test, t=3.049, df=4, p=0.038). The Δ*trf4*Δ*ctf18* strains have an average breakage rate of $0.842*10^{-6}$ (SEM=0.35) for the no repeat strains and an average breakage rate of $54.18*10^{-6}$ (SEM= 6.56).

The no repeat tract phenotypes for wild-type, Δ*trf4*, Δ*ctf18*, and Δ*trf4*Δ*ctf18* yeast strains are significantly different (ANOVA, df=3,8, F=11.695, p=0.003). *ΔTrf4Δctf18* has a significantly lower fragility rate than Δ*ctf18* (Bonferroni, α*=0.0167, p=0.0003), Δ*trf4* (p=0.0152), and the wild-type (p=0.038). The CAG-70 fragility rates are also significantly different (ANOVA, F=9.201, df=3,9, p=0.004). The Δ*trf4*Δ*ctf18* fragility rate is significantly higher than the wild-type (Bonferroni, α*=0.0167, p=0.00367). However, it is not significantly different from either the Δ*trf4* (p=0.167) or the Δ*ctf18* breakage rates (p=0.167).

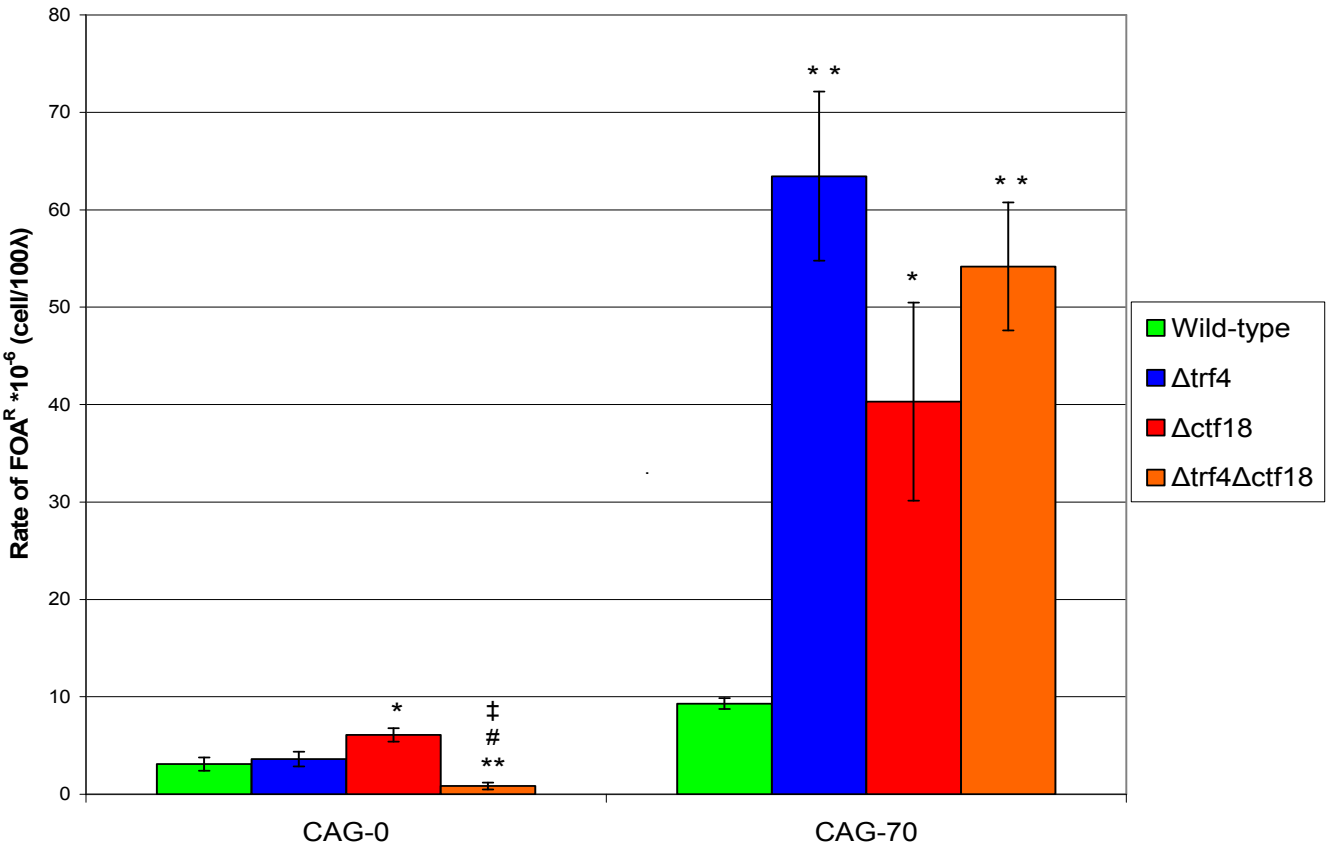

Figure 11. Δ*trf4*Δ*ctf18* Fragility Data Compared to Wild-type, Δ*trf4*, and Δ*ctf18*. Error bars represent the standard error of the mean (SEM). The * symbol indicates p<0.05 compared to the wild-type, and ** indicates p<0.01 (pooled variance t-test). ‡ denotes a significant difference from Δ*trf4*, while # denotes a significant difference from Δ*ctf18* (Bonferroni multiple comparisons test, p<α*).

Previous instability data from another lab member, Lionel Gellon, showed that Δ*ctf18* CAG-70 mutants are 35% contracted and 4.8% expanded, which is a significant 6 fold increase over the wild-type in contractions ($p=4.49*10^{-13}$) and not significant 1.8 fold increase in expansions (p=0.63). Δ*Trf4*Δ*ctf18* double mutants were found to be 31.7% contracted and 11.9% expanded (Fig 12). This is a significant 5.5 fold increase in contractions ($p=1.25*10^{-9}$) and a significant 14.9 fold increase in expansions over the wild-type ($p=1.3*10^{-5}$). This double-mutant also displays a significant increase in contractions (p= 0.0004) and expansions (p=0.016) over the Δ*trf4* mutant. Δ*Trf4*Δ*ctf18* is not significantly different than the Δ*ctf18* phenotype for contractions (p=0.68), but has a significantly greater phenotype for expansions (p=0.0011).

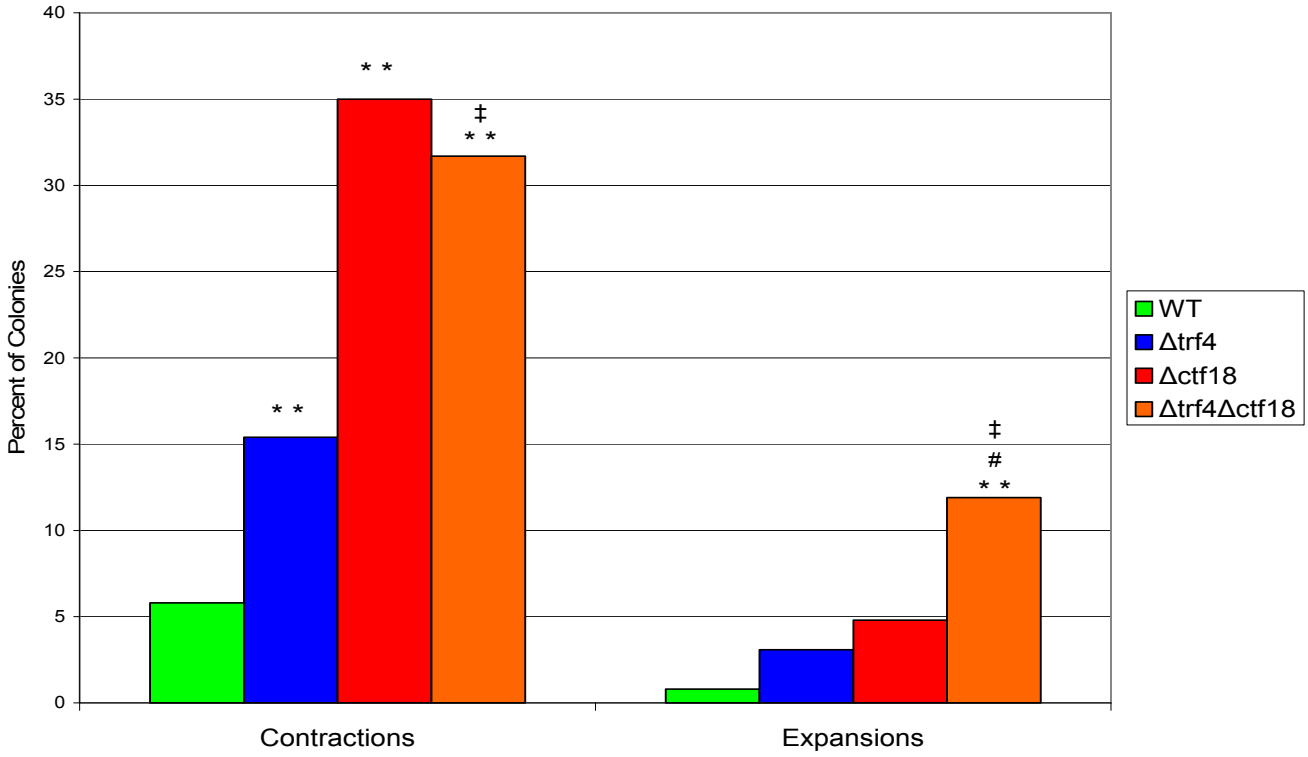

Figure 12. Δ*trf4*Δ*ctf18* Instability Data Compared to the Wild-type, Δ*trf4*, and Δ*ctf18*. The * symbol indicates p<0.05 in comparison to the wild-type, and ** indicates p<0.01 (Fischer's Exact Test). ‡ denotes a significant difference from Δ*trf4*, while # denotes a significant difference from Δ*ctf18* (Fischer's Exact Test).

Exploring the potential involvement of *TRF4* in the postreplication repair pathway

The genes *RAD5*, *RAD6,* and *RAD30* are all involved in the postreplication repair (PRR) pathway, which resolves stalled replication forks by allowing them to bypass sites of DNA damage (Myung& Smith 2008). There are two pathways for PRR in yeast, translesion synthesis (TLS) and template switching (TS) (Myung & Smith 2008). TLS is initiated by the monoubiquitination of PCNA by Rad6 and Rad18. The pathway bypasses damage by switching the replicative DNA polymerase for a TLS polymerase, such as pol η, which is coded by *RAD30.* The mechanism of the TS pathway is still poorly understood, but it is initiated by the polyubiquitination of PCNA by Rad5 (Myung & Smith 2008). This polyubiquitination step likely occurs after the monubiquitination of PCNA by Rad6 and Rad18 (Lee & Myung 2008). Since PRR has been implicated in CAG repeat maintenance (Daee et al 2007), we sought to determine whether *TRF4*'s role in preventing fragility and instability may be working through one of these PRR pathways. In order examine a potential role, Δ*trf4*Δ*rad5*, Δ*trf4*Δ*rad6*, and Δ*trf4*Δ*rad30* double mutants were assayed.

The Δ*rad5* fragility phenotype was determined by three assays carried out by Ranjith Anand, in addition to one assay that I carried out. The average breakage rate for Δ*rad5* is $3.51*10^{-6}$ (SEM= 0.74) for mutants with no repeat tract, and it is $9.81*10^{-6}$ (SEM=3.43) for mutants with 70 repeats. This phenotype represents no significant increase over the wild-type in either the no repeat strains (pooled t-test, t=0.442, p=0.682) or the CAG-70 strains (t=0.156, p=0.883). The Δ*trf4*Δ*rad5* mutants displayed a breakage rate of $19.8*10^{-6}$ (SEM= 2.09) when no repeat tract was present and a $64.29*10^{-6}$ (SEM= 5.87) for the CAG-70 tract mutants. The fragility rates for the no CAG tract wild-type, Δ*trf4*, and Δ*rad5*, and Δ*trf4*Δ*rad5* strains were significantly different (ANOVA, F=45.300, p<0.001). Further analysis showed that the

Δ*trf4*Δ*rad5* double mutant with no repeats had a significantly higher fragility rate than the wild-type (Bonferroni, α*=0.0167, p<0.00017), Δ*trf4* (p<0.00017), and Δ*rad5* (p<0.00017). The CAG-70 wild-type, Δ*trf4*, Δ*rad5,* and Δ*trf4*Δ*rad5* strains were also significantly different (ANOVA, F=24.087, df= 3,9, p<0.001). Additionally, the Δ*trf4*Δ*rad5* CAG-70 phenotype represents a significant increase in fragility over the wild-type (Bonferroni, α*=0.0167, p=0.00017) and Δ*rad5* (p=0.00033), but no significant increase over Δ*trf4* (p=0.167). (Figure 13)

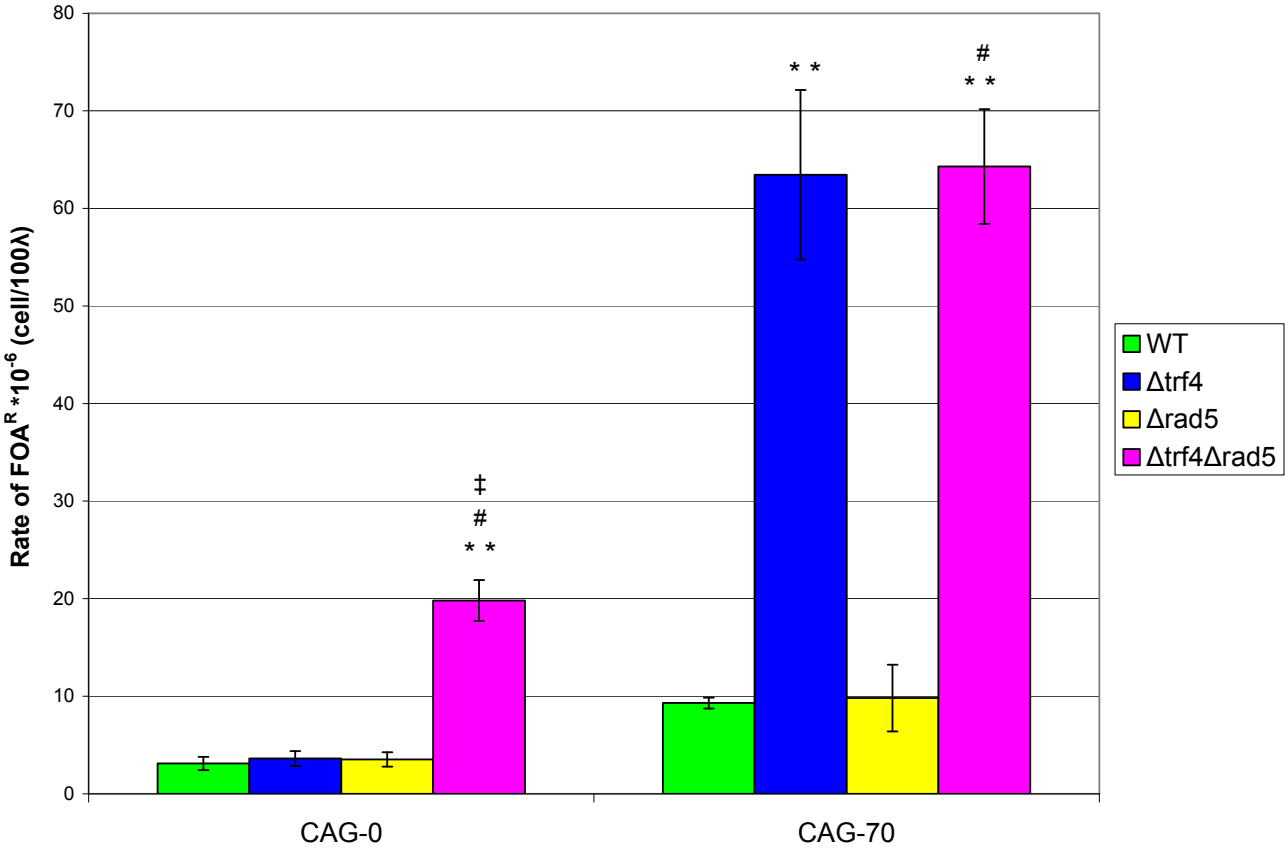

Figure 13. Δ*trf4*Δ*rad5* Fragility Data Compared to Wild-type, Δ*trf4*, and Δ*rad5*. Error bars represent the standard error of the mean (SEM). The * symbol indicates p<0.05 compared to the wild-type, and ** indicates p<0.01 (pooled variance t-test). ‡ denotes a significant difference from Δ*trf4*, while # denotes a significant difference from Δ*rad5* (Bonferroni multiple comparisons test, p<α*).

Δ*Rad5* instability data was a compilation of data collected by me (46 reactions) and Ranjith Anand (48 reactions). This mutant shows 5.3% contractions and 0% expansions, neither of which are statistically different than the wild-type phenotype (p=1, 1). The Δ*trf4*Δ*rad5* double-mutant displayed 8.65% contractions and 0.96% expansions. The contractions phenotype is not statistically different than wild-type (p=0.348), Δ*rad5* (p=0.416), or the Δ*trf4* phenotype (p=0.162). The expansions phenotype is not also statistically different than the wild-type (p=1), Δ*rad5* (p=1), or Δ*trf4* (p=0.385). (Figure 14)

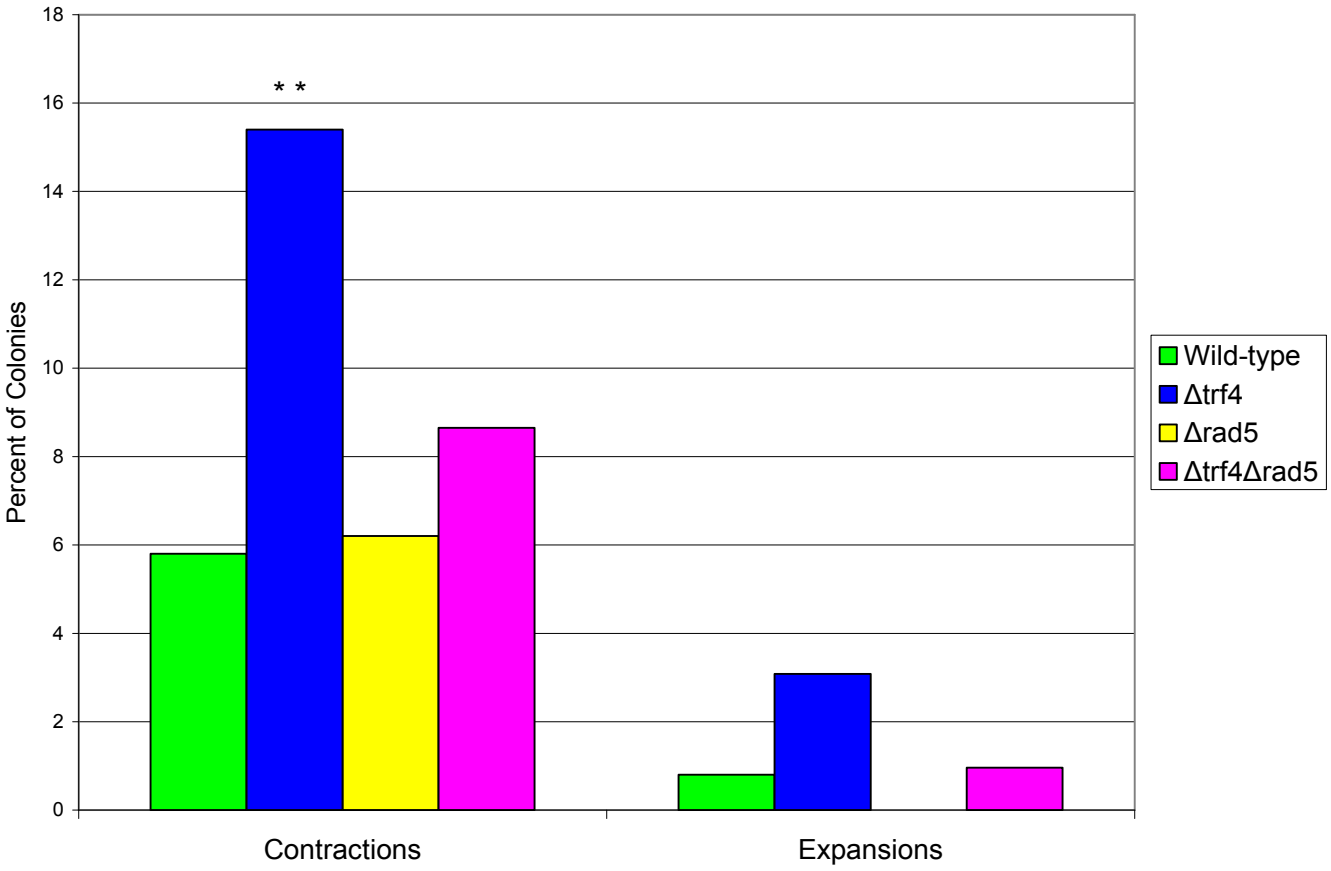

Figure 14. Δ*trf4*Δ*rad5* Instability Data Compared to the Wild-type, Δ*trf4,* and Δ*rad5*. The * symbol indicates p<0.05 in comparison to the wild-type, and ** indicates p<0.01 (Fischer's Exact Test). ‡ denotes a significant difference from Δ*trf4,* while # denotes a significant difference from Δ*rad5* (Fischer's Exact Test).

Δ*Rad30* mutants with no repeats display an average breakage rate of $5.96*10^{-6}$ (SEM=1.40), which is not significantly different than the wild-type phenotype (t=1.858, df=4, p=0.164). Δ*Rad30* strains with 70 repeats has a fragility rate of $11.51*10^{-6}$ (SEM=1.46), which is also not significantly different than wild-type yeast (t=1.434, df=4, p=0.225). The Δ*trf4*Δ*rad30* double mutant with 70 CAG repeats displayed a fragility rate of $80.18*10^{-6}$ (SEM=16.19). Statistical analysis showed that the wild-type, Δ*trf4*, Δ*rad30*, and Δ*trf4*Δ*rad30* CAG-70 strains differed in their fragility rates (ANOVA, F=11.068, df=3, 10, p=0.002). Further analysis showed that the Δ*trf4*Δ*rad30* double mutant shows significantly increased fragility over the wild-type (Bonferroni, α*=0.0167, p=0.001) and Δ*rad30* (p=0.0012). However, the double mutant's fragility did not significantly differ from Δ*trf4* (p=0.167). (Figure 15)

I was unable to obtain Δ*rad30* instability data due to an inability of the PCR procedure to give clear bands. 130 PCR reactions were performed and only 34 reactions showed any band on the gel. These bands were barely visible, making it difficult to discern potential contractions or expansions. However, the visible bands did not seem to be contracted or expanded, suggesting that Δ*rad30* has a phenotype close to wild-type. When the same PCR mix was used on 26 Δ*rad30* colonies and 25 Δ*rad6* colonies, the Δ*rad6* PCR products all showed very clear bands, and the Δ*rad30* reactions indistinct faint bands or not band at all (Figure 16). This suggests that the phenotype of this mutant disrupts the ability for our PCR procedure to isolate the CAG repeat fragment.

Figure 16. Δ*rad30*(70) vs. Δ*rad6*(70) instability gels

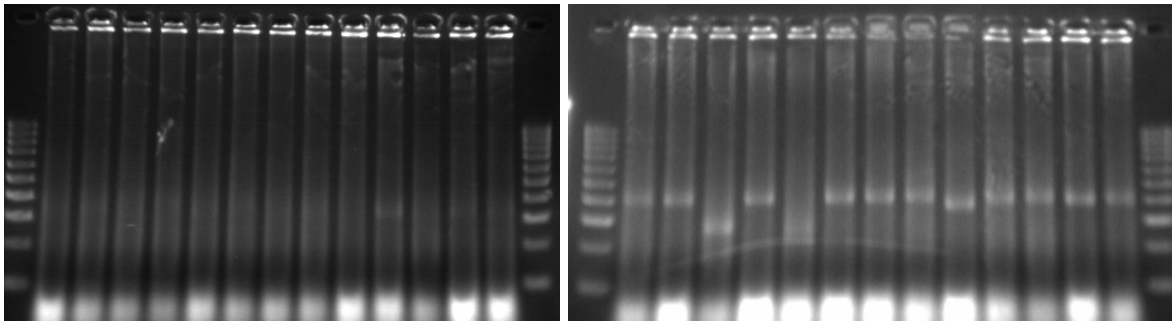

Δ*rad30*(70) Δ*rad6*(70)

The Δ*trf4*Δ*rad30* double mutant was able to give clear PCR bands, so instability data was collected for these strains. The double mutant displayed 13.5% contractions, which is a significant 2.3 fold increase over the wild-type (p=0.029). However, this phenotype was not significantly different than Δ*trf4* (p=0.71). Δ*Trf4*Δ*rad30* also showed 3.85% expansions. Though this represents a 4.8 fold increase over the wild-type, this increase is not significant (p=0.069). This expansions phenotype was also not significantly different than Δ*trf4* (p=1). (Figure 17)

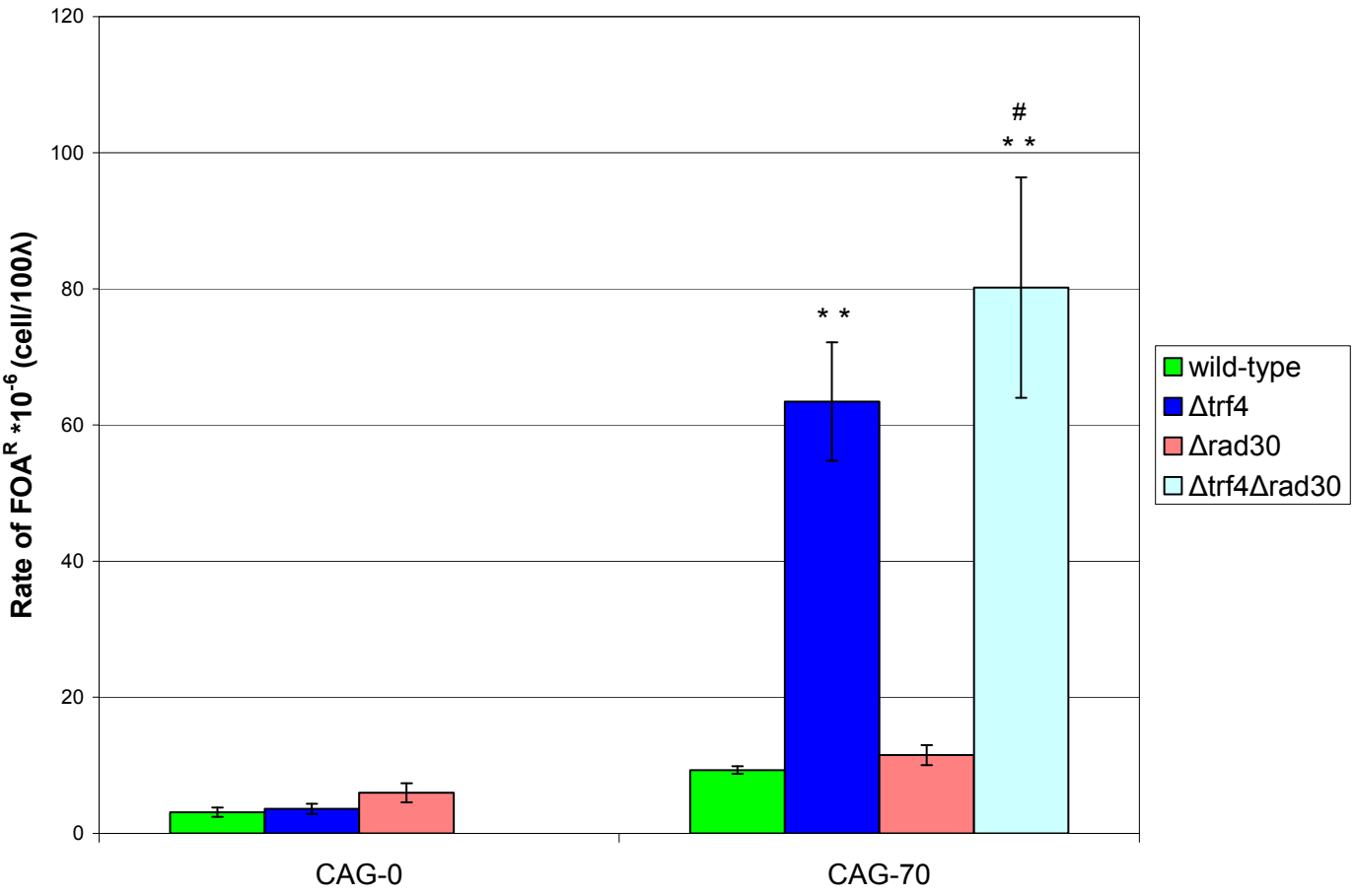

Figure 15. Δ*trf4*Δ*rad30* Fragility Data Compared to Wild-type, Δ*trf4*, and Δ*rad30*. Error bars represent the standard error of the mean (SEM). The * symbol indicates $p<0.05$ compared to the wild-type, and ** indicates $p<0.01$ (pooled variance t-test). ‡ denotes a significant difference from Δ*trf4*, while # denotes a significant difference from Δ*rad30* (Bonferroni multiple comparisons test, $p<\alpha^*$).

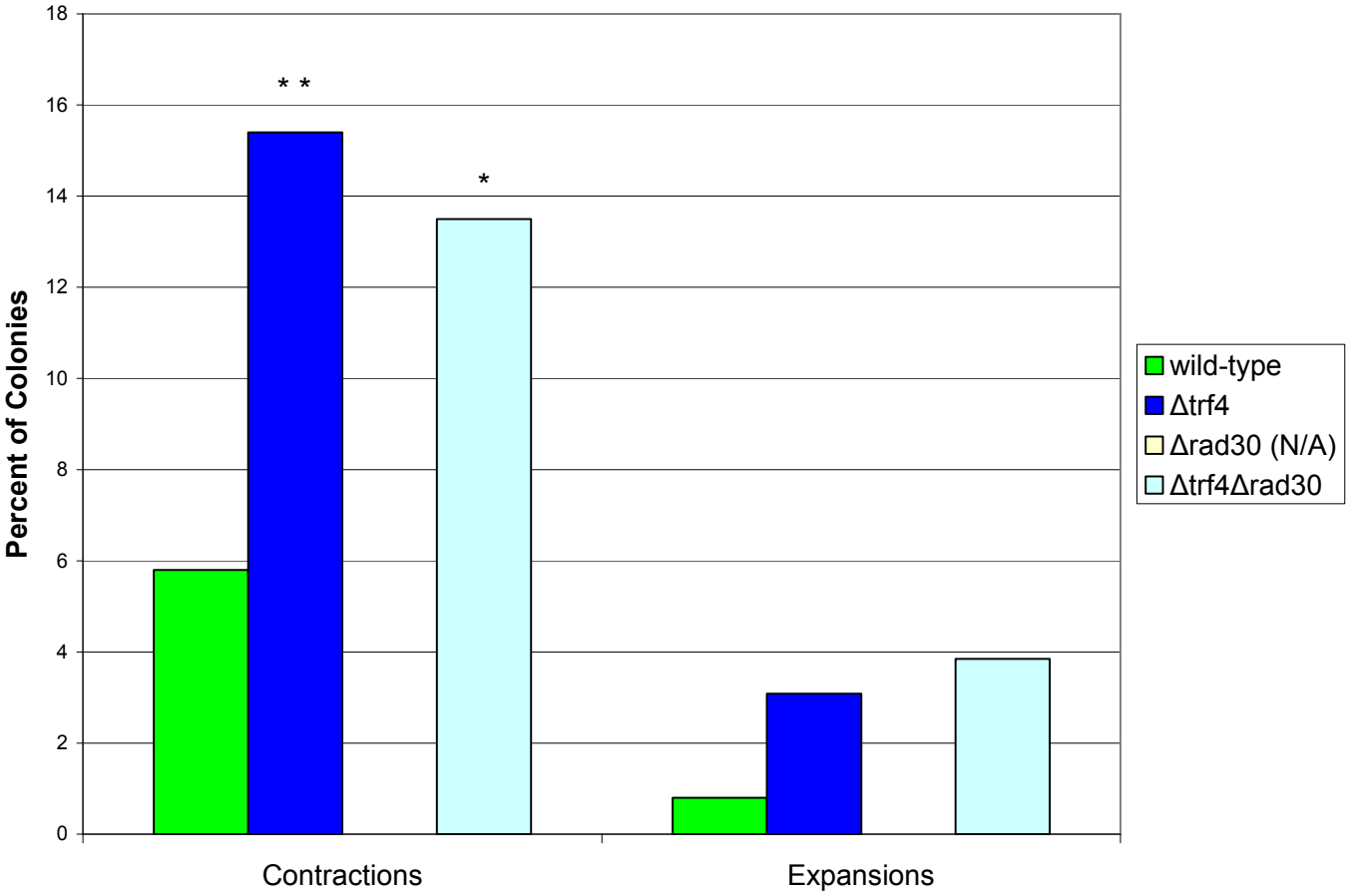

Figure 17. Δ*trf4*Δ*rad30* Instability Data Compared to the Wild-type and Δ*trf4*. The * symbol indicates $p<0.05$ in comparison to the wild-type, and ** indicates $p<0.01$ (Fischer's Exact Test). ‡ denotes a significant difference from Δ*trf4* (Fischer's Exact Test). Δ*rad30* data was not attained due to a propensity for failed PCR reactions in this strain.

Δ*Rad6* mutants lacking CAG repeats displayed an average breakage rate of $3.4*10^{-6}$ (SEM= 1.15), which is not significantly different from the wild type (pooled variance t-test, t=0.250, df=4, p=0.815). *Rad6* strains containing 70 CAG repeats had an average breakage rate of $7.97*10^{-6}$ (SEM=0.22). This rate was also not significantly different than the wild-type rate (t=-2.139, df=4, p=0.099). The Δ*trf4*Δ*rad6* CAG-70 double mutant has a breakage rate of $11.30*10^{-6}$(Figure 18). Statistical analysis showed that the fragility rates for the wild-type, Δ*trf4*,

Δ*rad6,* and Δ*trf4*Δ*rad6* were statistically different. (ANOVA, F=26.115, df=3,9, p<0.001) The fragility rate for Δ*trf4*Δ*rad6* was not significantly different than the wild-type (Bonferroni, α*=0.0167, p=0.167) or Δ*rad6* (p=0.167). However, the fragility rate of the double mutant was significantly decreased from Δ*trf4* (p=0.00017).

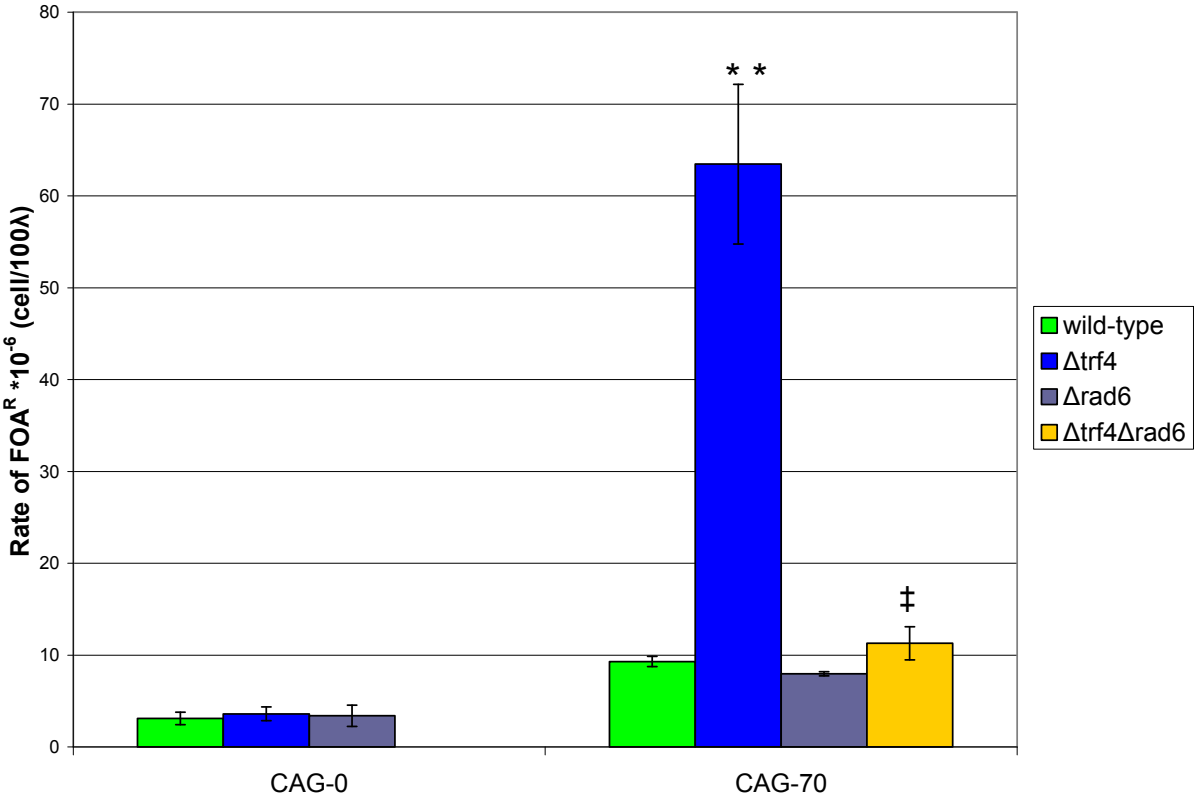

Figure 17. Δ*trf4*Δ*rad36* Fragility Data Compared to the Wild-type, Δ*trf4*, and Δ*rad6*. Error bars represent the standard error of the mean (SEM). The * symbol indicates p<0.05 compared to the wild-type, and ** indicates p<0.01 (pooled variance t-test). ‡ denotes a significant difference from Δ*trf4*, while # denotes a significant difference from Δ*rad30*

The Δ*rad6* mutant with 70 CAG repeats displayed 8.0% contractions and 3.0% expansions. The contractions phenotype is not significantly increased from the wild-type (p=0.47), and while the expansions represent a 3.8 fold increase over the wild-type, this increase is also not significant (p=0.151). Instability data for the Δ*trf4*Δ*rad6* mutant was unable to be

obtained. This mutant showed the same phenotype as Δ*trf4*Δ*rad30* and PCR on this mutant did not produce any product, even when a positive control did show a band. (Figure 19)

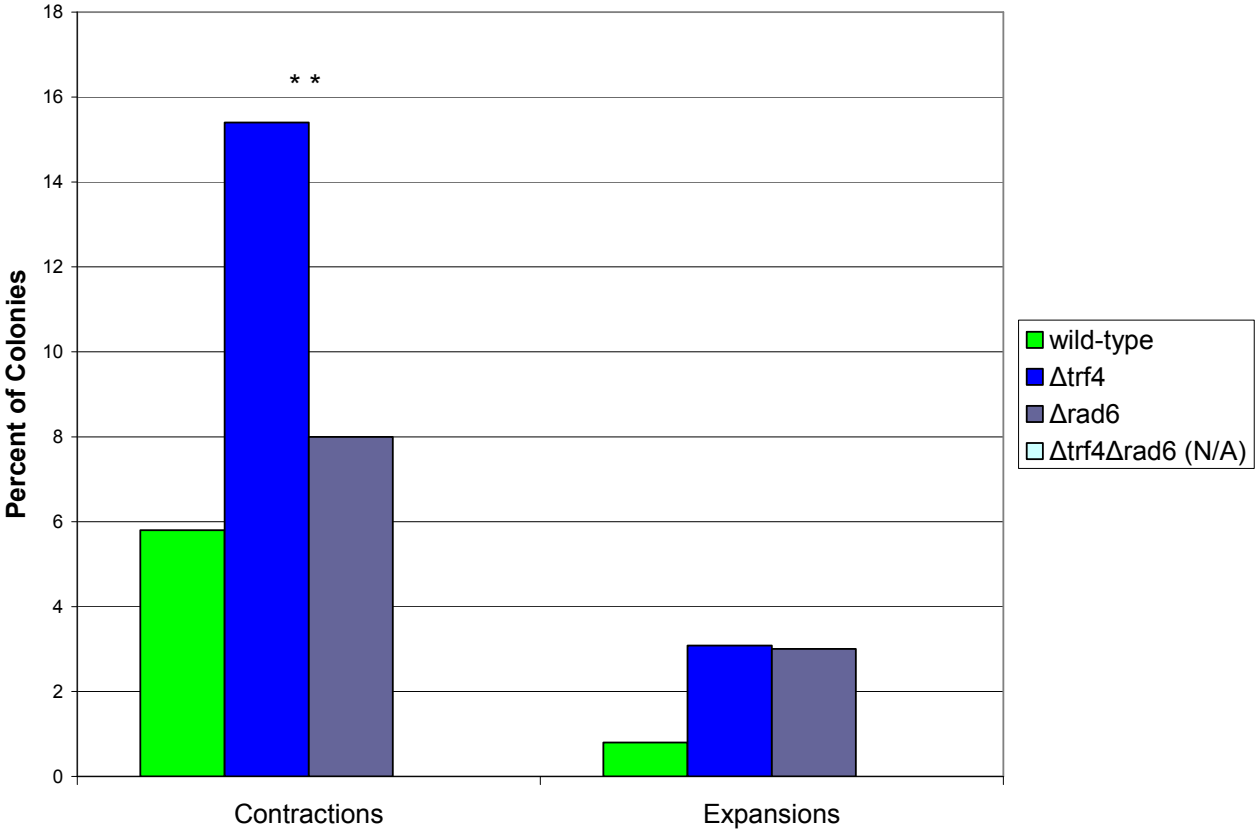

Figure 19. Δ*trf4 and* Δ*rad6* Instability Data Compared to the Wild-type. The * symbol indicates $p<0.05$ in comparison to the wild-type, and ** indicates $p<0.01$ (Fischer's Exact Test).

Figure 20. Fragility Summary

	CAG-0				CAG-70			
Strain	Average Breakage Rate*10^{-6}	SEM	P	Fold/ WT	Average Breakage Rate*10^{-6}	SEM	P	Fold/ WT
Wild-type	2.65	0.68			7.61	0.56		
Δ*trf4*	3.61	0.75	0.620	1.36	63.45	8.69	0.003	8.34
Δ*trf5*	4.77	0.29	0.082	1.8	12.38	1.76	0.169	1.63
Δ*ctf18*	6.1	0.68	0.033	2.3	40.3	10.17	0.038	5.30
Δ*trf4*Δ*ctf18*	0.842	0.35	0.038	0.32	54.18	6.56	0.00378	7.12
Δ*rad5*	3.51	0.74	0.682	1.32	9.81	3.43	0.883	1.29
Δ*trf4*Δ*rad5*	19.8	2.09	<0.00017	7.47	64.29	5.87	0.00017	8.45
Δ*rad52*	5.3	0.6	0.182	2	24.35	1.3	0.002	3.20
Δ*trf4*Δ*rad52*	4.1	1.82	0.167	1.55	121.18	24.94	0.00017	15.92
Δ*rad30*	5.96	1.40	0.164	2.25	11.51	1.46	0.225	1.51
Δ*trf4*Δ*rad30*	N/A	---	---	---	80.18	16.19	0.001	10.54
Δ*rad6*	3.4	1.15	0.815	1.28	7.97	0.22	0.099	1.05
Δ*trf4*Δ*rad6*	N/A	---	---	---	11.30	1.80	0.167	1.48

Figure 21. Instability Summary

	Medium Tract (CAG-70)						
	Contractions			Expansions			n
	%	Fold/WT	P-value	%	Fold/WT	P-value	
Wild-type	5.8			0.8			243
Δ*trf4*	15.4	2.7	0.0039	3.08	3.9	0.189	130
Δ*trf5*	5.2	0.9	1	2.6	3.3	0.245	77
Δ*ctf18*	35	6.0	4.49e-13	12.5	15.6	8.01e-7	144
Δ*trf4*Δ*ctf18*	31.7	5.5	1.25e-9	11.9	14.9	1.3e-5	101
Δ*rad5*	5.3	0.9	1	0	0	1	94
Δ*trf4*Δ*rad5*	8.65	1.5	0.35	0.96	1.2	1	104
Δ*rad52*	10.7	1.8	0.107	1.4	1.8	0.307	140
Δ*trf4*Δ*rad52*	17.3	3.0	0.0018	2.9	3.6	0.16	104
Δ*rad30*	N/A	-	-	N/A	-	-	-
Δ*trf4*Δ*rad30*	13.5	2.3	0.029	3.85	4.8	0.069	104
Δ*rad6*	8.0	1.4	0.47	3.0	3.8	0.151	100
Δ*trf4*Δ*rad6*	N/A	-	-	N/A	-	-	-

RnaseH Experiment

In order to ensure that the RNaseH and control plasmids sent to us were in fact what we desired, restriction enzyme digests were performed. First, plasmids were digested with SacI (Figure 22). This digestion was intended to cut all of the plasmids once, linearizing them. The plasmid containing the RnaseH gene was expected to be 855 base-pairs longer than the control plasmid (Gaidamakov et al 2005). However, there was no observable size-difference between the plasmids. Instead, both plasmids were about 8000 base-pairs long, and this size corresponds to the expected size of the control plasmid of 7760 base-pairs.

Figure 22. SacI Digest. Lanes 1 and 3 contain the plasmid labeled to contain the RNaseH gene, while lanes 2 and 4 contain the control plasmid. The plasmids digested in lanes 1 and 2 are digested directly from the original tubes sent to us. The plasmids in lanes 3 and 4 are the digested products of the transformation of the plasmids into bacteria in order to replicate the plasmid.

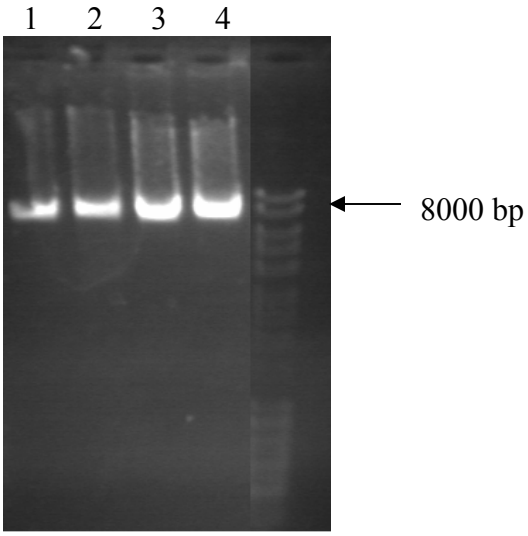

Next, a digestion was carried out on these two original plasmids using EcoRI, since this was the restriction enzyme supposedly used to clone in the RNase H gene (Figure 23). This restriction enzyme was expected to cut the control plasmid at two restriction sites, one in the multiple cloning site and one in the LEU2 marker, giving expected bands that are 2305 and 5455 base-pairs long. If the other plasmid in fact contains RNaseH, this restriction enzyme should

release the gene by cutting on either side of it, and it should also cut in the LEU2 marker, giving an expected three bands or 2305, 5455, and 855 base-pairs. The digestion products for both plasmids gave two bands, at about 6kb and 2.5kb. This showed that neither of the plasmids sent to us actually contained the RNaseH gene and both plasmids are likely control plasmids.

Figure 23. EcoRI Digest. Lane 1 contains the plasmid thought to contain the RNaseH gene, and lane 2 contains the control plasmid.

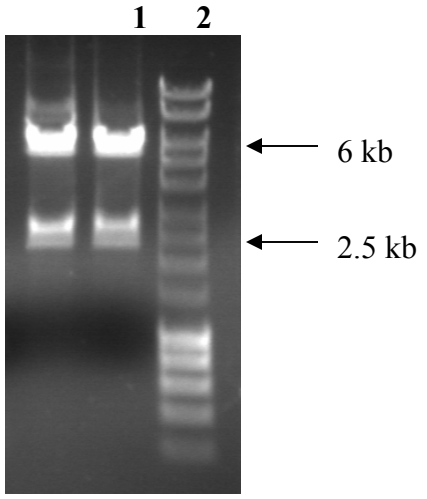

Next, the LEU2 marker in the control plasmid was switched for a TRP1 marker and the plasmid was transformed into both wild-type and Δ*trf4* yeast containing a CAG-70 YAC. The plasmids were isolated from eight of these strains, four from the wild-type and four from Δ*trf4*. A Cla1 digestion was run on these plasmids with the original plasmids as controls to ensure that they were in fact disrupted with TRP1 (Figure 24). There is a Cla1 restriction site within the multiple cloning site of this plasmid, and additionally there is a Cla1 restriction site within the LEU2 marker but not the TRP1 marker. Therefore, this restriction enzyme was expected to cut the original plasmids twice, forming bands that are 1808 and 5952 base-pairs long. The TRP1-containing plasmids were only expected to be cut once, with an expected size for the linearized plasmids of 6527 base-pairs. The original LEU2 plasmids showed bands at the expected sizes. The plasmids isolated from the transformations all showed a lack of the 1808bp band, as

expected. However, while some plasmids showed a band size of about 6.5kb, some others had a band size of around 5.5kb. All of the plasmids contained only one band however, showing that they no longer contained the LEU2 marker. The strains with the 5.5kb band size were discarded, and only strains containing the 6.5kb band size were used to run assays.

Figure 24. ClaI Digestion. Lane 1 contains the original plasmid thought to contain RNaseH, and lane 2 contains the original control plasmid. Lanes 3-6 contain plasmids isolated from the Δ*trf4* strains after the transformation to switch the LEU2 marker for a TRP1 marker. Lanes 7-10 contain plasmids isolated from the wild-type strains after the transformation to switch the markers.

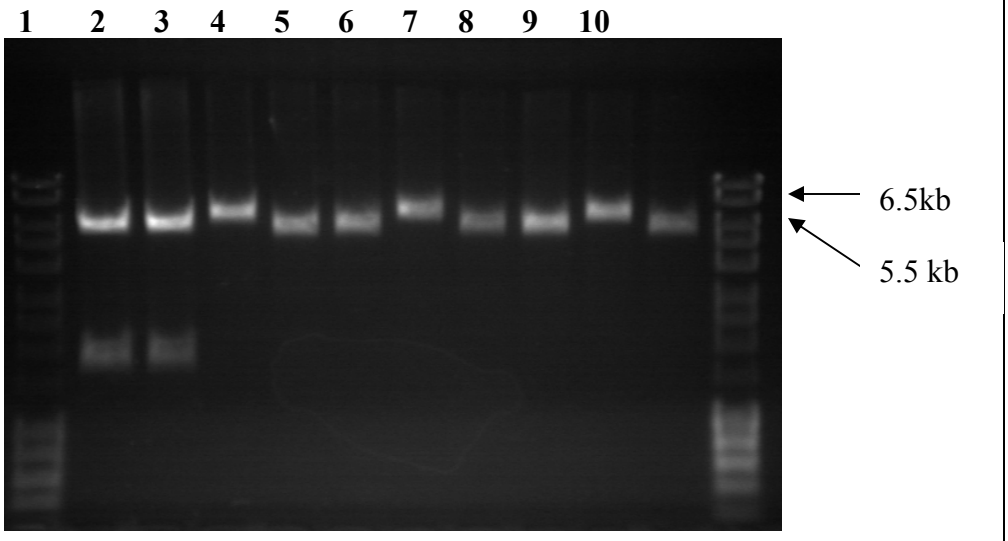

One strain of wild-type CAG-70 yeast containing the control plasmid and two strains of Δ*trf4* CAG-70 yeast containing the control plasmid were isolated. Three fragility assays were performed on these strains (Figure 25). The wild-type yeast with the plasmid had an average rate of FOA resistance of $54.78 * 10^{-6}$ (SEM=4.88). The Δ*trf4* strains containing this plasmid had an average rate of FOA resistance of $264 * 10^{-6}$ (SEM=81.27). The wild-type with the plasmid had a significantly increased FOA^R rate over the wild-type rate when no plasmid is present (pooled variance t-test, df=4, t=-9.266, p=0.001). The Δ*trf4* strain containing the plasmid also displayed a significantly increased FOA^R rate over the Δ*trf4* rate without the plasmid (pooled variance t-test,

t=-2.454, df=6, p=0.05). This increased rate of FOA resistance is likely not due to actual breakage events in the chromosome and instead is a result of integration events of the plasmid and the URA3 gene in the YAC. This type of event has also been observed in past experiments attempted with plasmids and our YAC system. This result led us to abandon the planned experiment because a change in the fragility phenotype due to the presence of RNaseH would be difficult to confirm when the control plasmid in itself has such an effect on the rate of FOA resistance.

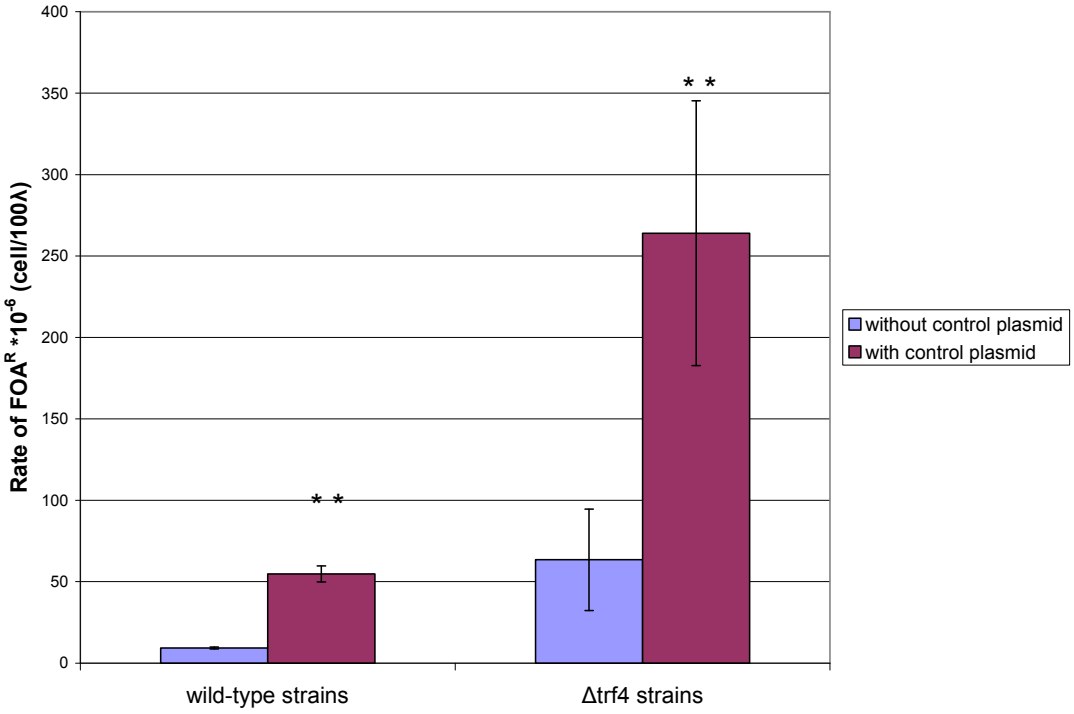

Figure 25. Rate of FOA^R for wild-type and Δ*trf4* strains with and without the control plasmid. Error bars represent the standard error of the mean (SEM). * indicates $p<0.05$ in comparison to the strain without the plasmid, and ** indicates $p<0.01$ (pooled variance t-test).

Preliminary instability calculations were performed to see if the control plasmid has a similar effect on instability due to its potential for integration with the YAC (Figure 26). 21 reactions were performed in the wild-type strain containing the control plasmid. 33.3% of the

colonies displayed a contracted phenotype while 4.8% of the colonies were expanded. The contraction phenotype is significantly higher than the wild-type without the plasmid (Fisher's Exact Test, p=0.0004) while the expansion phenotype is not significantly different (p=0.22). 45 reactions were performed for the Δ*trf4* background containing the control plasmid. 22.2% of colonies were contracted and 0% were expanded. However, although the contraction phenotype is increased when the plasmid is present, this is not statistically significant (p=0.36), and the expansions phenotype is also not statistically different (p=0.57). More reactions would have to be carried out with both strains in order to determine the actual instability phenotype, but these preliminary results indicate that this background is not optimal for use with the plasmid for determining instability.

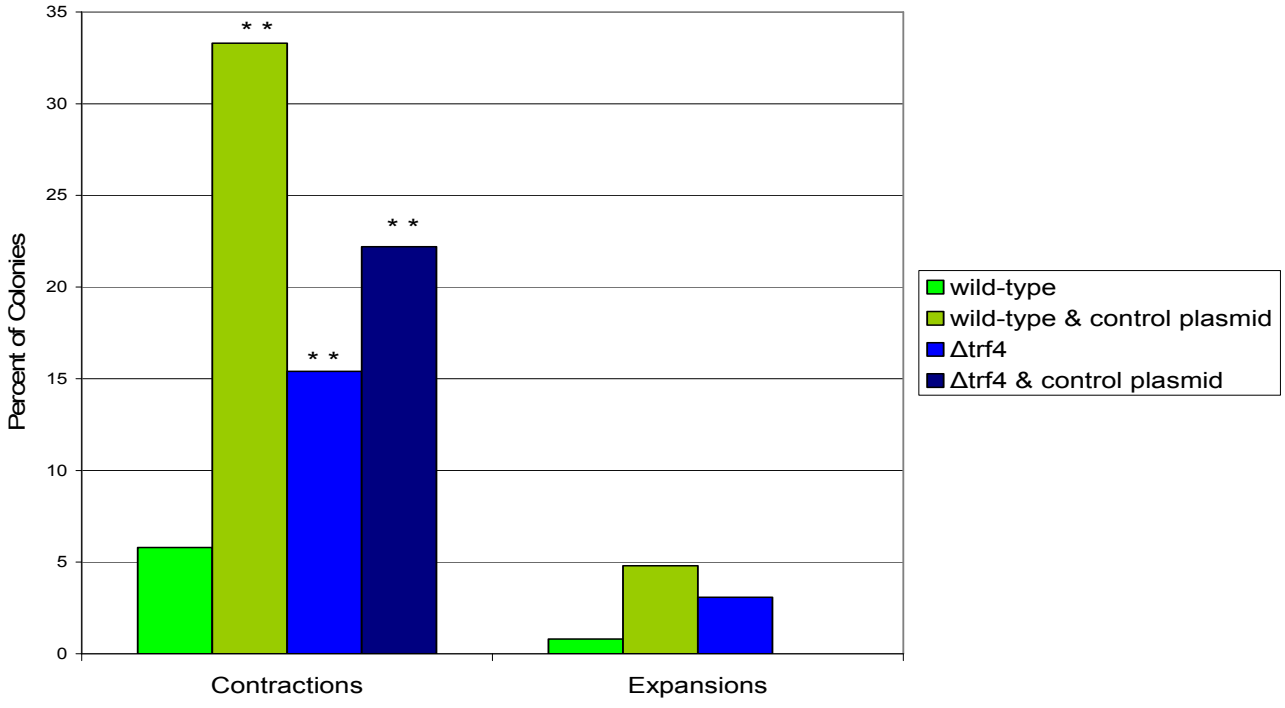

Figure 26. Instability Data for wild-type and Δ*trf4* strains with and without the control plasmid. * indicates p<0.05 compared to the wild-type without a plasmid, and ** indicates p<0.01.

Conclusion

The initial goal of my project was to determine if the gene *TRF4* plays a role in the maintenance of trinucleotide repeat regions. The increased fragility in Δ*trf4* over wild-type yeast, which is specific to strains containing CAG repeats, suggests that trf4p plays some role in preventing breakage in repetitive sequences in the genome. *TRF4* mutants also show increased instability in repeat tract length, particularly increased contractions. This suggests that trf4p functions to keep CAG repeat regions stable in length.

Unlike Δ*trf4*, Δ*trf5* displays no increase in fragility or instability over the wild-type. *TRF5* is a functional homologue of *TRF4,* and these two genes seem to perform some overlapping functions. However, some differences have been observed between Δ*trf4* and Δ*trf5* mutants, such as differences in drug sensitivities, and the TRAMP4 and TRAMP5 complexes have been observed to target some different substrates (Egecioglu et al 2006). *TRF4*'s role in the prevention of fragility and instability in trinucleotide repeat regions does not seem to be shared by *TRF5*.

In order to determine if Δ*trf4*'s fragility and instability phenotypes could be attributed to a role in double stranded break repair, a Δ*trf4*Δ*rad52* double mutant was assayed. Since there was no significant difference in fragility among the wild-type, either single mutant, or the double mutant when no repeats were present, *TRF4* and *RAD52* likely do not affect fragility in the absence of a CAG repeat tract. For strains containing 70 CAG repeats, the Δ*trf4*Δ*rad52* phenotype was significantly greater than both the Δ*trf4* and Δ*rad52* single mutants, displaying an additive pattern. This suggests that both Δ*trf4* and Δ*rad52* are involved in the prevention of fragility in CAG repeat tracts, but in two separate pathways.

In the instability assay, neither *RAD52* or *TRF4* seem to be having any preventative effect on expansions of CAG repeats, as neither single mutant or the double mutant show a significant effect on the expansions phenotype over the wild-type. Alternatively, Δ*rad52*, Δ*trf4*, and Δ*trf4*Δ*rad52* all show increased contractions over the wild-type. The double-mutant's phenotype is not significantly increased from either Δ*trf4* or Δ*rad52*, suggesting that these two genes may be working in the same pathway to prevent instability of repeat tracts, particularly repeat contractions.

Since the Ctf18-RFC has been shown to influence CAG repeat fragility and instability, likely through a fork stabilization model (Lionel Gellon, unpublished data), and *TRF4* and *CTF18* have been shown to interact through a synthetic growth defect (Pan et al 2005), a Δ*trf4*Δ*ctf18* double mutant was assayed to elucidate a possible role for *TRF4* in the Ctf18 pathway. When no repeat tract is present, the Δ*trf4*Δ*ctf18* double mutant shows a suppression in fragility rate from both single mutants and the wild-type. This suggests that without a repeat tract, *TRF4* must be present in order for Δ*ctf18* to display its increased fragility phenotype. In other words, *TRF4* could be actually mediating increased fragility, but only when the genome lacks *CTF18* and no repeats are present. In the strains containing 70 CAG repeats, the Δ*trf4*Δ*ctf18* double mutant displays increased fragility over the wild-type. However, the double-mutant's fragility phenotype is not significantly different than either the Δ*trf4* or Δ*ctf18* single mutants. This epistatic relationship suggests that *TRF4* and *CTF18* are working in the same pathway to prevent fragility in repeat tracts.

In the instability assay, the Δ*trf4*Δ*ctf18* mutant displays significantly increased contractions and expansions over the wild-type. Contractions and expansions are also significantly increased over the Δ*trf4* single mutant, but are not significantly different than the

Δ*ctf18* phenotype. Since the contractions phenotype is not additive, once again, *TRF4* and *CTF18* seem to be working in the same pathway. Here, since the double mutant phenotype matches the Δ*ctf18* phenotype and is increased from Δ*trf4*, *CTF18* seems to be working upstream of *TRF4* in the same epistatic pathway to prevent contractions of CAG repetitive tracts. The Δ*trf4*Δ*ctf18* expansions phenotype is synergistic to the Δ*trf4* and Δ*ctf18* single mutant phenotypes, suggesting that these two genes are preventing expansions in two partially redundant separate pathways.

Although little is still known about this role of the Ctf18-RFC in preventing repeat fragility and instability, one proposed model is that the complex is able to stabilize stalled replication forks through its PCNA loading and unloading function (Lionel Gellon, unpublished data). My fragility and instability data suggests that *TRF4* may be involved in this pathway. While *TRF4*'s DNA polymerase role has been disputed, this data seems to point to some action of trf4 on a DNA-level.

In order to explore a potential role for *TRF4* in the post-replication repair pathway, Δ*trf4*Δ*rad5*, Δ*trf4*Δ*rad6*, and Δ*trf4*Δ*rad30* double mutants were created. Interestingly, though previous research had implicated PRR-related proteins in the maintenance of short CAG repeats (Daee et al 2007), none of our single mutants for *RAD5, RAD6,* or *RAD30* showed any effect on repeat fragility or instability over the wild-type.

When no repeat tract was present, the Δ*trf4*Δ*rad5* double mutant showed increased fragility over the wild-type and both the Δ*trf4* and Δ*rad5* single mutants. This additive, or potentially synergistic, relationship suggests that these genes are working in separate pathways to prevent DNA fragility in the absence of a repeat tract. If the double mutant phenotype is in fact synergistic, this suggests that the two separate pathways are at least partially redundant. In the

strains containing 70 CAG repeats, the double mutant's fragility phenotype was significantly increased from the wild-type and the Δ*rad5* phenotype, but it was not significantly different than the Δ*trf4* mutant. Since Δ*rad5* does not display increased fragility over the wild-type in a CAG-70 background, we are unable to determine whether the double mutant's phenotype is additive between Δ*trf4* and Δ*rad5* (indicating two separate pathways), if it represents *TRF4* working upstream of *RAD5* epistatically to prevent fragility, or if *RAD5* has no role in repeat fragility. However, considering that the Δ*rad5* single mutant shows no increased fragility when 70 CAG repeats are present, *TRF4* seems to play a greater role in CAG breakage repair than *RAD5*, and *TRF4*'s role is likely not working though the TS pathway which requires *RAD5*.

In the instability assay, the Δ*trf4*Δ*rad5* double mutant actually seems to display a suppression of the Δ*trf4* contractions phenotype. The Δ*trf4*Δ*rad5* mutant's contraction phenotype matches that of the wild-type and the Δ*rad5* single mutant, while the Δ*trf4* single mutant showed a significant increase in contractions over the wild-type. Though suppression in the contractions phenotype appears to be occurring in the double mutant, the Δ*trf4*Δ*rad5* contractions mutant is actually not significantly lower than Δ*trf4*, preventing us from knowing what is actually occurring. If the double mutant is decreasing the amount of contractions over what is observed in Δ*trf4* single mutants, this would suggest that *TRF4* and *RAD5* are working in the same pathway to prevent instability, but *RAD5* is working upstream of *TRF4*. In order for *TRF4* to function in this pathway, *RAD5* must also be present, though the gene *RAD5* on its own does not prevent repeat instability. Alternatively, since Δ*trf4*Δ*rad5* is not significantly different than Δ*trf4*, *TRF4* and *RAD5* may be working together to prevent fragility in a pathway in which *TRF4* is working upstream of *RAD5,* or *RAD5* may have no role in repeat contractions. The expansions phenotype shows no significant difference between the wild-type, Δ*trf4,* Δ*rad5*, and

Δ*trf4*Δ*rad5,* though it seems to follow the same pattern as the contractions with a depression of the Δ*trf4* instability when Δ*rad5* is deleted simultaneously. In order to make any conclusions about this pathway, more instability reactions need to be performed in order to determine if the double mutant matches the phenotype of Δ*trf4* or Δ*rad5*. However, since the instability phenotype of the double mutant does not seem to be additive, *TRF4* and *RAD5* may be working in the same pathway to mediate CAG repeat instability.

Δ*Rad6* strains both with no CAG tract and 70 CAG repeats were created in order to do a double mutant experiment with *TRF4*. Issues with transformation and primers created difficulty in the isolation of a Δ*trf4*Δ*rad6* mutant, but two double mutant strains were recently created, and fragility and instability assays are currently underway. The results of these experiments will provide insight into whether *TRF4* may be preventing CAG repeat fragility and instability through involvement in the TLS pathway.

The Δ*trf4*Δ*rad30* double mutant with 70 CAG repeats displayed a fragility phenotype that was significantly increased over the wild-type and Δ*rad30,* but not significantly different than the Δ*trf4* phenotype. This suggests that *RAD30* either has no effect on chromosome fragility or is working to prevent fragility in a pathway downstream of *TRF4*. However, if *RAD30* is involved in the prevention of fragility downstream of *TRF4*, we would expect that the single mutant deletion of this gene would show increased fragility, so it is unlikely that *TRF4* and *RAD30* are working in the same pathway. However, since *RAD30* codes for just one of several translesion polymerases, this result does not rule out a role for *TRF4* in the TLS pathway in general.

Instability data for the Δ*rad30* mutant was not attained due to difficulty in using the PCR technique to replicate the CAG tracts in this strain. Clear bands did not appear on the gel and this

effect seems to be strain specific. Although the length of the few visible bands suggests that Δ*rad30* yeast have a similar instability phenotype to wild-type yeast, no definite conclusions can be drawn. Interestingly, Δ*trf4*Δ*rad30* strains displayed no difficulty with PCR. One model for this phenotype is that the *RAD30* may be involved in repair of damage in CAG repeats, and when it is missing, damage in the repeat tracts creates difficulty in our PCR polymerase's function. However, *TRF4* must be present for this damage to occur because when this gene is deleted there is no barrier to the PCR polymerase's function and PCR proceeds as expected. This theory is counter to my data, which suggests that *TRF4* prevents fragility and instability and is potentially involved in DNA repair. Further experiments are necessary to elucidate what is actually occurring in the Δ*rad30* strain. First of all, since only one Δ*rad30* CAG-70 strain was originally created and all of the assays were run on this strain, another mutant should be created. If this second Δ*rad30* mutant also has a phenotype of PCR difficulty, a potential further experiment could be to either sequence the CAG tracts in the Δ*rad30* yeast strains or look at the tracts by Southern blot to see if they are disrupted by any damage. A double mutant of Δ*rad30* and some gene other than *TRF4* could also be created to determine if the issues with PCR are resolved similarly to the Δ*trf4*Δ*rad30* mutants.

The Δ*trf4*Δ*rad30* yeast displayed a significant increase in contractions and a nonsignifcant increase in expansions over the wild-type. The instability phenotypes were also not significantly different than Δ*trf4* strains. Though no direct conclusions can be made due to the lack of Δ*rad30* instability data, either *RAD30* is not involved in the maintenance of CAG stability or is working with *TRF4* but downstream in this pathway.

Figure 27. Summary of Fragility Conclusions.

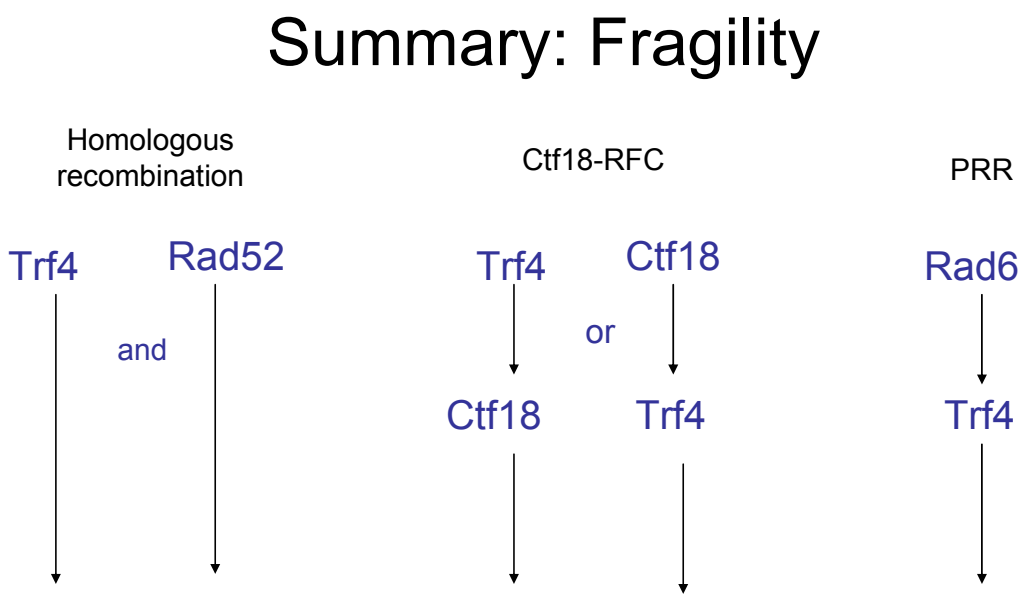

Figure 28. Summary of Instability Conclusions.

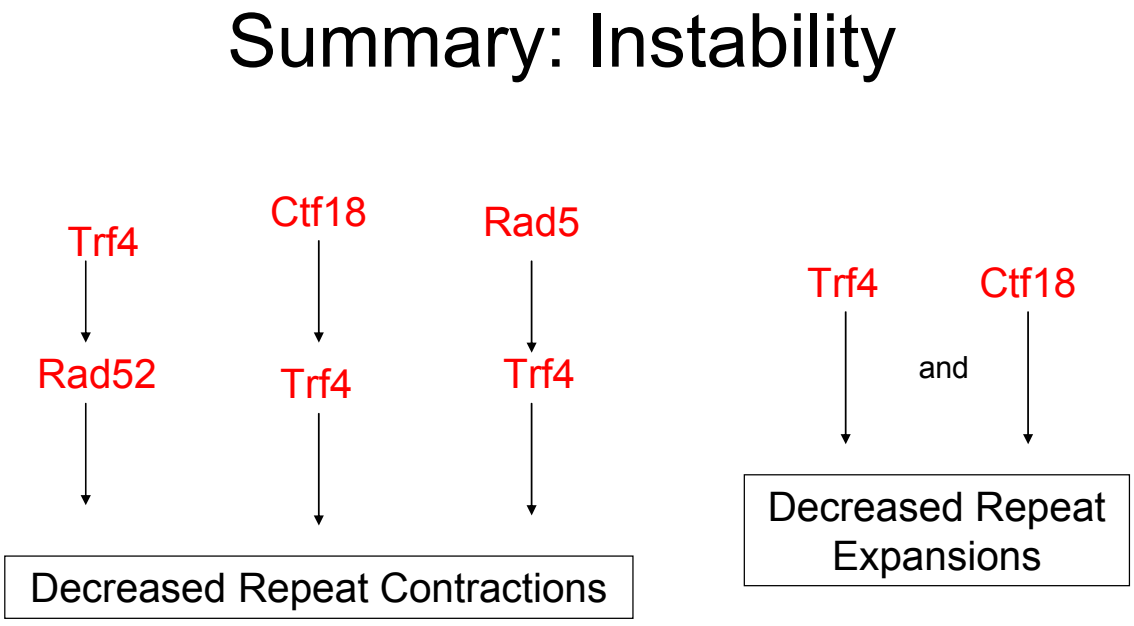

The RNaseH experiment is an important component of this project because it will allow us to determine if RNA:DNA hybrids play any effect in the observed Δ*trf4* phenotypes. It will assay whether the RNA-level role of *TRF4* in the TRAMP complex may be influencing our YAC system. By targeting RNAs for destruction, trf4p may destroy RNAs that could otherwise interact with the repeat sequences, particularly at the replication fork, to cause fragility and instability. However, my preliminary fragility and instability data with the control plasmid not containing RNaseH showed that the presence of this plasmid has a large effect on fragility and instability in our YAC background, which challenges the possibility that the RNaseH experiment would give interpretable results. For this reason, we will instead run this experiment in another yeast background that has not interacted with plasmids in the past, like our YAC system has been shown to do. This background contains a tract of CAG repeats on the yeast chromosome instead of a YAC. After Δ*trf4* data is collected in this background, the control plasmid and a plasmid containing RNaseH will be cloned in. Assays will also be run with both plasmids in the wild-type. Our hope is that the effect of the presence or absence of RNaseH will be observable, since the plasmid itself should not have an effect on instability.

Overall, my data shows that deleting the gene *TRF4* leads to increased fragility and instability in CAG repeat tracts, while deleting *TRF5* does not have this effect. Though I have not yet been able to fully discern the pathway by which *TRF4* is affecting repeat fragility and instability, my genetic experiments have provided some insight into its potential role. In the prevention of repeat fragility, *TRF4* seems to be functioning in a separate pathway from *RAD52*'s double-stranded break repair pathway. However, these two genes may be working in the same pathway to prevent repeat instability, particularly repeat contractions. *TRF4* may be working in the same pathway as the Ctf18-RFC to prevent both fragility and instability of

repeats. It is unclear whether *TRF4* is preventing CAG fragility and instability through the PRR pathway, but since none of the single mutants for PRR related genes showed any effect on repeat instability or fragility, it is likely that *TRF4*'s role is independent of PRR. However, my data does suggest a link between *TRF4* and *RAD5* in the prevention of instability. Though more instability reactions need to be carried out to establish statistical significance, Rad5 seems to be working upstream of Trf4 in this pathway.

An important next step for this project is to determine whether Δ*trf4*'s RNA-level role as a component of the TRAMP complex is playing any role in its fragility and instability phenotypes. We hope to accomplish this via our planned RnaseH experiment. Though we do not expect transcription of the CAG tract in our YAC system, it will be important to determine whether this is actually occurring, especially if the presence of DNA:RNA hybrids seems to be influencing Δ*trf4*'s phenotype.

If *TRF4*'s RNA-level role is not found to be the major determinant of its mutant phenotype, more experiments on the DNA level will be carried out. Further double-mutants with repair proteins can provide insight into which repair mechanism(s) trf4 is participating in. For example, a Δ*trf4*Δ*apn1*Δ*apn2* triple mutant would examine *TRF4*'s potential involvement in base excision repair, as suggested by the discovery trf4's dRP-lyase activity (Gellon 2008). Additionally, in order to determine whether *TRF4*'s potential role in cohesion is affecting DNA fragility and instability, a Δ*trf4*Δ*smc1* or Δ*trf4*Δ*smc2* double mutant could be assayed. Since *TRF4* seems to have some involvement in the PRR pathway, we would also like to carry out experiments with mutants defective for monoubiquitination and polyubiquitination of PCNA. Finally, we would like to carry out a 2D assay to see if Δ*trf4* mutants show increased fork stalling and a CHIP assay to see if trf4p is physically located at the CAG repeat sequence.

TRF4's potential role in repeat maintenance has exciting implications, both in the field of repeat stability and in the understanding of the highly disputed role of *TRF4*.

Works Cited

Allmang, C., Kufel, J., Chanfreau, G., Mitchell, P., Petfalski, E., & D. Tollervey. (1999) "Functions of the exosome in rRNA, snoRNA, and snRNA sythesis." *The EMBO Journal*. 18:5399-5410.

Anderson, J. (2005) "RNA turnover: unexpected consequences of being tailed." *Current Biology*. 15(16): R635-638.

Bermudez, V., Y. Maniwa, I. Tappin, K. Ozato, K. Yokomori, and J. Hurwitz. (2003) "The alternative Ctf18-Dcc1-Ctf8-replication factor C complex required for sister chromatid cohesion loads proliferating cell nuclear antigen onto DNA." *PNAS*. 100:18, 10237-10242.

Callahan, J., Andrews, K., Zakain, V., & C. Freudenreich. (2003) "Mutations in yeast replication proteins that increase CAG/CTG expansions also increase repeat fragility." *Molecular and Cellular Biology*. 23(21): 7849-7860.

Carson, D. and M. Christman. (2001) "Evidence that replication fork components catalyze establishment of cohesion between sister chromatids." *PNAS*. 98:15, 8270-8275.

Castano, I., Brzoska, P., Sadoff, B., Chen, H., & M. Christman (March 1996) "Mitotic chromosome condensation in the rDNA requires *TRF4* and DNA topoisomerase I in *Saccharomyces cerevisiae*." *Genes Dev*. 10: 2564-2576.

Castano, I., Heath-Pagliusi, S., Sadoff, B., Fitzhugh, D., & M. Christman. (April 1996) "A novel family of *TRF* (DNA topoisomerase I-related function) genes required for proper nuclear segregation." *Nucleic Acids Research*. 24,12: 2404-2410.

Daee, D., T. Mertz, & R. Lahue. (2006) "Postreplication Repair Inhibits CAG CTG Repeat Expansions in *Saccharomyces cerevisiae*." 27(1):102-110.

Edwards, S., C.M. Li, D.L. Levy, J. Brown, P.M. Snow, and J.L. Campbell. (2003) "Saccharomyces cerevisiae DNA polymerase epsilon and polymerase sigma interact physically and functionally, suggesting a role for polymerase epsilon in sister chromatid cohesion." *Molecular Cell Biology*. 23:8, 2733-48.

Egecioglu, D., Henras, A., & G. Chanfreau, G. (2006) "Contributions of Trf4p- and Trf5p-dependent polyadenylation to the processing and degradative functions of the yeast nuclear exosome." *RNA*. 12:26-32.

Freudenreich, C. and M. Lahiri. (2004) "Structure-Forming CAG/CTG Repeat Sequences are Sensitive to Breakage in the Absence of Mrc1 Checkpoint Function and S-phase Checkpoint Signaling: Implications for Trinucleotide Repeat Expansion Diseases." *Landes Bioscience*. 3:11, 1370-1374.

Gaidamakov, S., Gorshkova, I., Schuck, P., Steinbach, P., Yamada, H., Crouch, R., & Cerretelli, S. (2005) "Eukaryotic Rnases H1 act processively by interactions through the duplex RNA-binding domain." *Nucleic Acids Research.* 33(7):2166-2175.

Gellon, L., Carson, D., Carson, J., & B. Demple. (2008) "Intrinsic 5'-Deoxyribose-5-phosphate Lyase Activity in *Saccharomyces cerevisiae* Trf4 Protein with a Possible Role in Base Excision DNA Repair." *DNA Repair*. 7(2): 187-198.

Hanna, J., E. Kroll, V. Lundbland, and F. Spencer. (2001) "*Saccharomyces cerevisiae* CTF18 and CTF4 Are Required for Sister Chromatid Cohesion." *Molecular and Cellular Biology*. 21:9, 3144-3158.

Haracska, L., Johnson, R., Prakash, L., & S. Prakash. (2005) "Trf4 and Trf5 Proteins of *Saccharomyces cerevisiae* Exhibit Poly(A) RNA Polymerase Activity but No DNA Polymerase Activity." *Molecular and Cellular Biology*. 25(22): 10183-10189.

Hoffman & Winston. (1987) "A ten-minute DNA preparation from yeast efficiently releases autonomous plasmids from transformation of *E. coli*." *Gene*. 57:267-272.

Houseley, J. & D. Tollervey. (2008) "The nuclear RNA surveillance machinery: The link between ncRNAs and genome structure in budding yeast?" *Biochimica et Biophysica Acta.* 1779: 239-246.

Houseley, J., Kotovic, K., Hage, A., & D. Tollervey. (2007) "Trf4 targets ncRNAs from telomeric rDNA spacer rehions and functions in rDNA copy number control." *EMBO*. 26(24): 4996-5006.

Huertas, P. & A. Aguilera. (2003) "Cotranscriptionally formed RNA:DNA hybrids mediate transcription elongation impairment and transcription-associated recombination." *Molecular Cell*. 12(3):711-721.

Kadaba, S., Krueger, A., & T. Trice. (2004) "Nuclear surveillance and degradation of hypomodified initiator $tRNA^{Met}$ in *S. cerevisiae*." *Genes Dev.* 18:1227-1240.

Lahiri, M., Gustafson, T., Majors, E., & C. Freudenreich. (2004) "Expanded CAG repeats activate the DNA damage checkpoint pathway." *Molecular Cell*. 15(2):287-293.

Lahue, R. & D. Slater. (2003) "DNA Repair and Trinucleotide Repeat Stability." *Frontiers in Biocscience*. 8:s653-665.

Lee, K. & K. Myung. (2008) "PCNA Modifications for Regulation of Post-Replication Repair Pathways." *Mol. Cells.* 26: 5-11.

Libri, D. (2010) "Nuclear Poly(A)-Binding Proteins and Nuclear Degradation: Take the mRNA and Run?" *Molecular Cell*. 37: 3-5.

Lui, Y., Prasad, R., Beard, W., Kedar, P., Hou, E., Shock, D., and S. Wilson. (2007) "Coordination of Steps in Single-nucleotide Base Excision Repair Mediated by

Apurinic/Apyrimidinic Endonuclease 1 and DNA Polymerase β." *J. Biol Chem. 282*,18:13532-13541.

Mirkin, E. & S. Mirkin. (2007) "Replication Fork Stalling at Natural Impediments." *Microbiology and Molecular Biology Reviews.*" 71(1):13-35.

Myung, K. & S. Smith. (2008) "The RAD5-dependent Postreplication Repair Pathway is Important to Suppress Gross Chromosomal Rearrangements." *J Natl Cancer Inst Monogr.* 39:12-15.

Neil, H., Malabat, C., d'Aubenton-Carafa, Y., Xu, Z., Steinmetz, L., & A. Jaquier. (2009) "Widespread biodirectional promoters are the major source of cryptic transcripts in yeast." *Nature*. Letters: 1-6.

Pan X., Ye P., Yuan D.S., Wang X., Bader J.S., Boeke J.D. (2006) A DNA integrity network in the yeast Saccharomyces cerevisiae. *Cell.* 124(5):1069-81

Petronczki, M., Chwalla, B., Siomos, M., Yokobayashi, S., Helmhart, W., Deutschbauer, A., Davis, R., Watanabe, Y., & K. Nasmyth. (2004) "Sister-chromatid cohesion mediated by the alternative RF-$C^{Ctf18/Dcc1/Ctf8}$, the helicase Chl1and the polymerase-α-associated protein Ctf4 is essential for chromatid disjunction during meiosis II." *Journal of Cell Science.* 117(16):3547-3559.

Reis, C. & J. Campbell. (2007) "Contribution of Trf4/5 and the Nuclear Exosome to Genome Stability Through Regulation of Histone mRNA Levels in *Saccharomyces cerevisiae*." *Genetics*. 175: 993-1010.

Sadoff, B., Heath-Pagliuso, S., Castano, I., Zhu, Y., Kieff, F., & M. Christman. (1995) "Isolation of Mutants of Saccharomyces cermisiae Requiring DNA Topoisomerase I." *Genetics.* 141: 465-479.

Saitoh, S., Chabes, A., McDonald, W., Thelander, L., Yates, J., & P. Russell. (2002) "Cid13 is a cytoplasmic poly(A) polymerase that regulates ribonuclease reductase mRNA." *Cell.* 109(5): 563-573.

Sundararajan, R., Gellon, L., Zunder, R., & C. Freudenreich. (2009) "Double-Strand Break Repair Pathways Protect against CAG/CTG Repeat Expansions, Contractions and Repeat-Mediated Chromosomal Fragility in *Saccharomyces cerevisiae*." *Genetics*. 184:65-77.

Symington, L. (2002) "Role of RAD52 Epistasis Group Genes in Homologous Recombination and Double-Strand Break Repair" *Microbiol. Mol. Biol. Rev.* 66(4): 630-669.

Uhlamann, F. (2000) "Chromosome Cohesion: a polymerase for chromosome bridges." *Current Biology*. 10(19): R698-R77.

Walowsky, C., Fitzhugh, D., Castano, I., Ju, J., Levin, N., & M. Christman. (1999) "The Topoisomerase-related Function Gene *TRF4* Affects Cellular Sensitivity to the Antitumor Agent Camptothecin." *The Journal of Biological Chemistry*. 242(11): 7302-7308.

Wang, Z., I. Castano, C. Adams, C. Yu, D. Fitzhugh, and M. Christman. (2002) "Structure/ Function Analysis of the *Saccharomyces cerevisiae* Trf4/Pol σ DNA Polymerase." *Genetics*. 160: 381-391.

Wang, Z., Castano, I., De Las Penas, A., Adams, C., & M. Christman. (2000) "Pol κ: A DNA Polymerase Required for Sister Chromatid Cohesion." *Science*. 289: 774-789.

Appendix A: Fragility Data for all Mutants. Error bars represent the standard error of the mean (SEM). The * symbol indicates $p<0.05$ compared to the wild-type, and ** indicates $p<0.01$ (pooled variance t-test). ‡ denotes a significant difference from Δ*trf4*, while # denotes a significant difference from the other single mutant (Bonferroni multiple comparisons test, $p<\alpha^*$).

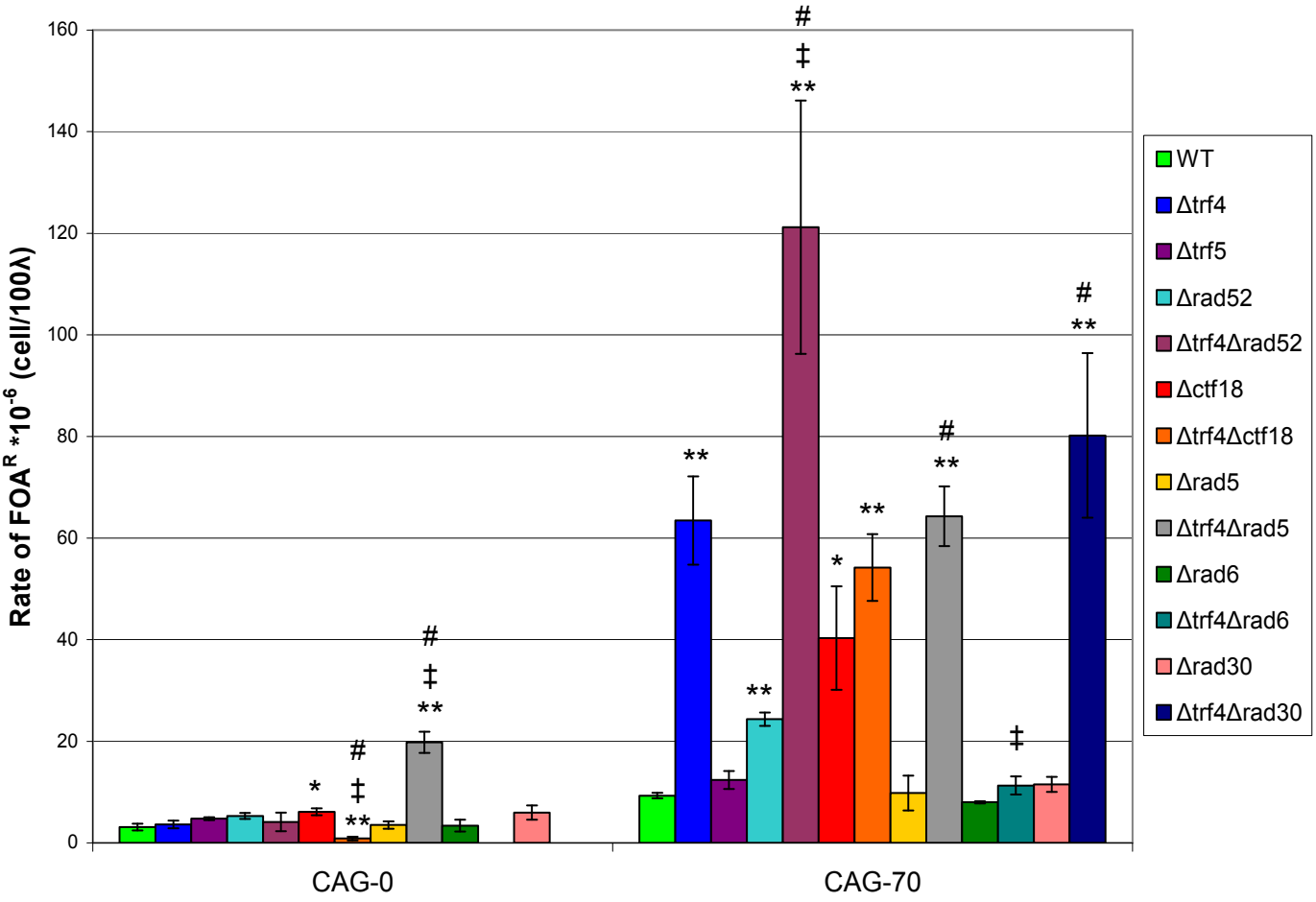

Appendix B: Fragility Data for Δ*trf4*Δ*rad52* and Δ*trf4*Δ*ctf18*. Error bars represent the standard error of the mean (SEM). The * symbol indicates $p<0.05$ compared to the wild-type, and ** indicates $p<0.01$ (pooled variance t-test). ‡ denotes a significant difference from Δ*trf4*, while # denotes a significant difference from the other single mutant (Bonferroni multiple comparisons test, $p<\alpha^*$).

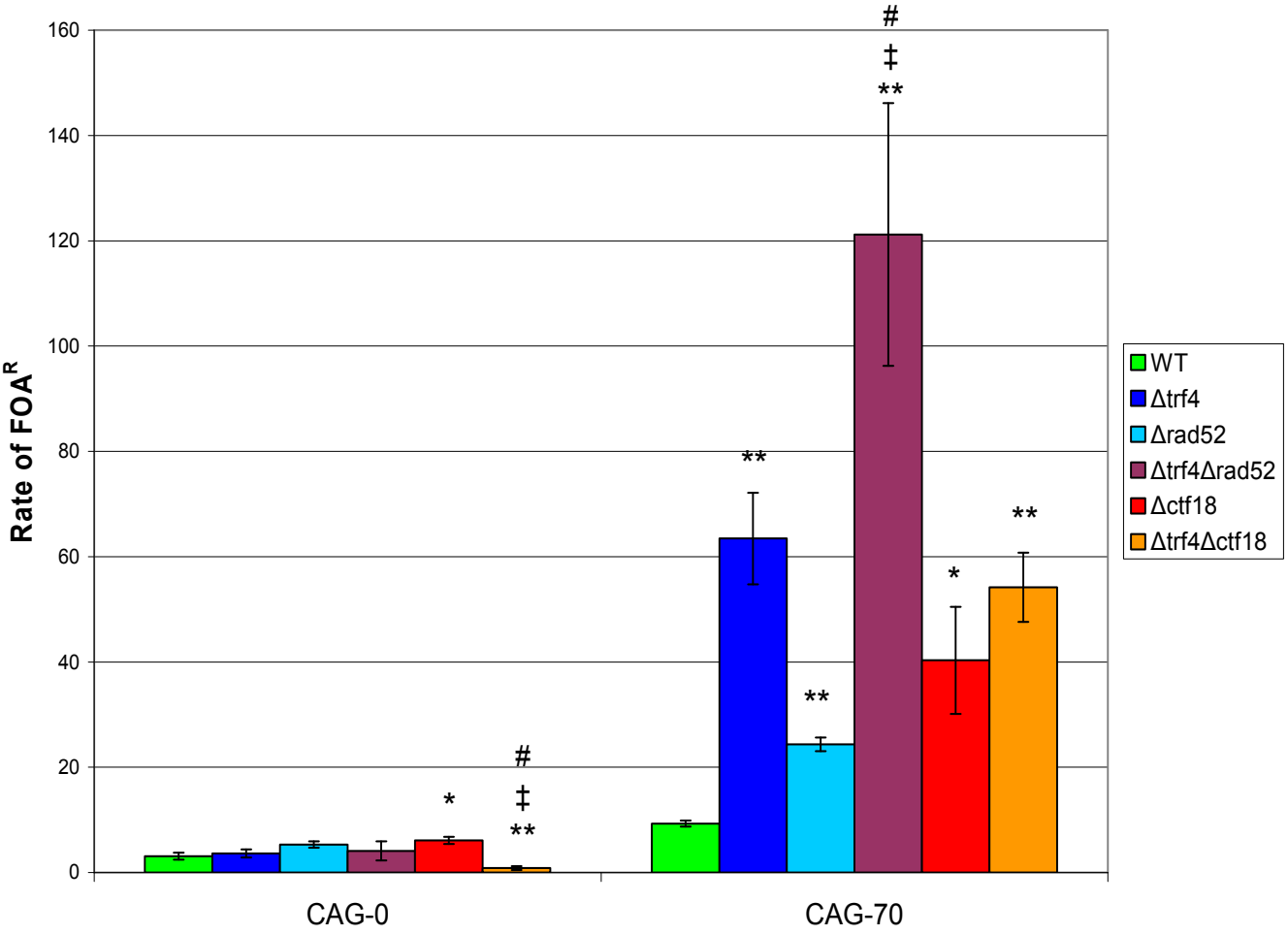

Appendix C: Fragility Data for Postreplication Repair Mutants. Error bars represent the standard error of the mean (SEM). The * symbol indicates $p<0.05$ compared to the wild-type, and ** indicates $p<0.01$ (pooled variance t-test). ‡ denotes a significant difference from Δ*trf4*, while # denotes a significant difference from the other single mutant (Bonferroni multiple comparisons test, $p<\alpha^*$).

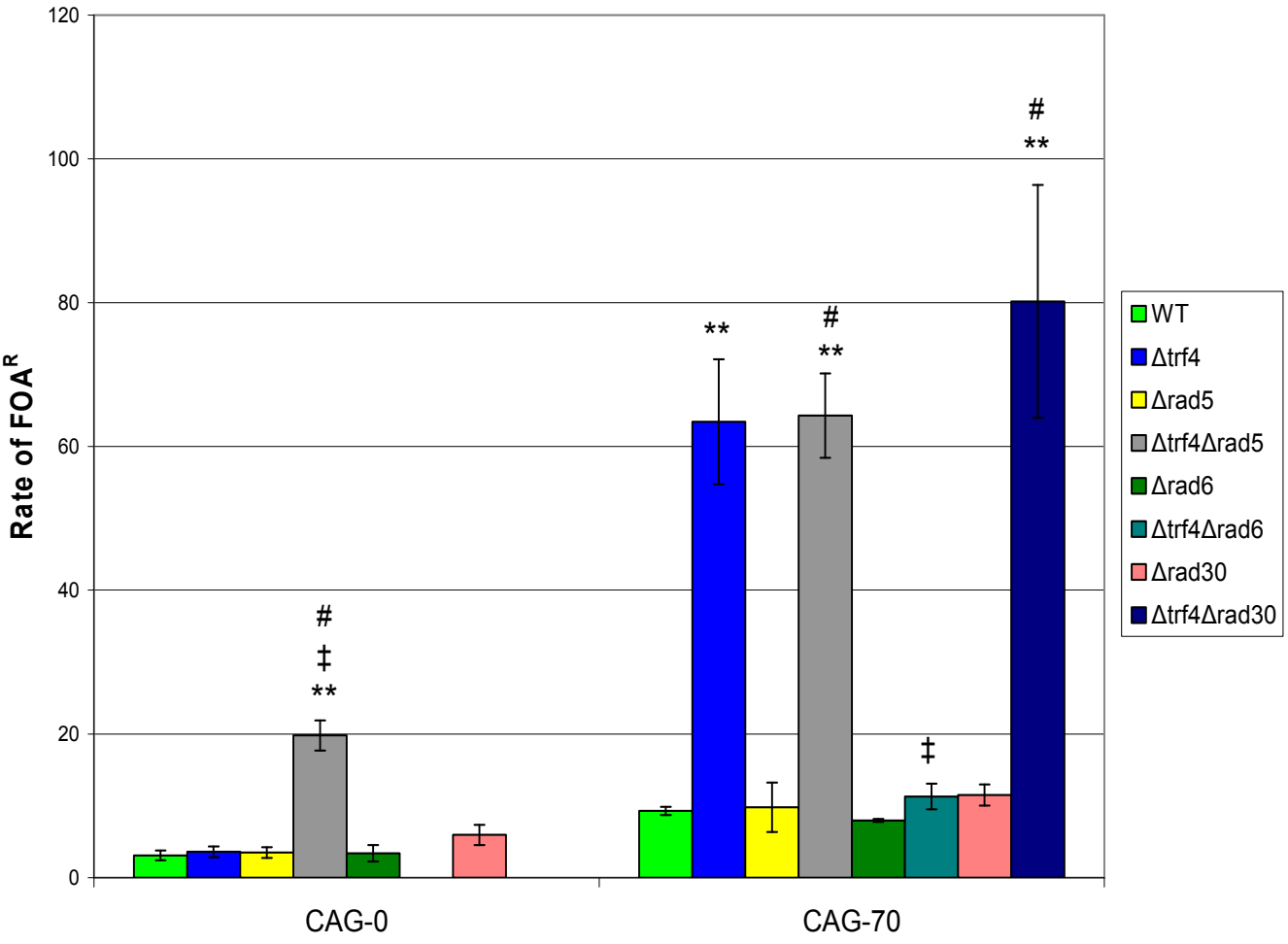

Appendix D: Instability Data for all Mutants. The * symbol indicates $p<0.05$ in comparison to the wild-type, and ** indicates $p<0.01$ (Fischer's Exact Test). ‡ denotes a significant difference from Δ*trf4*, while # denotes a significant difference from the other single mutant (Fischer's Exact Test).

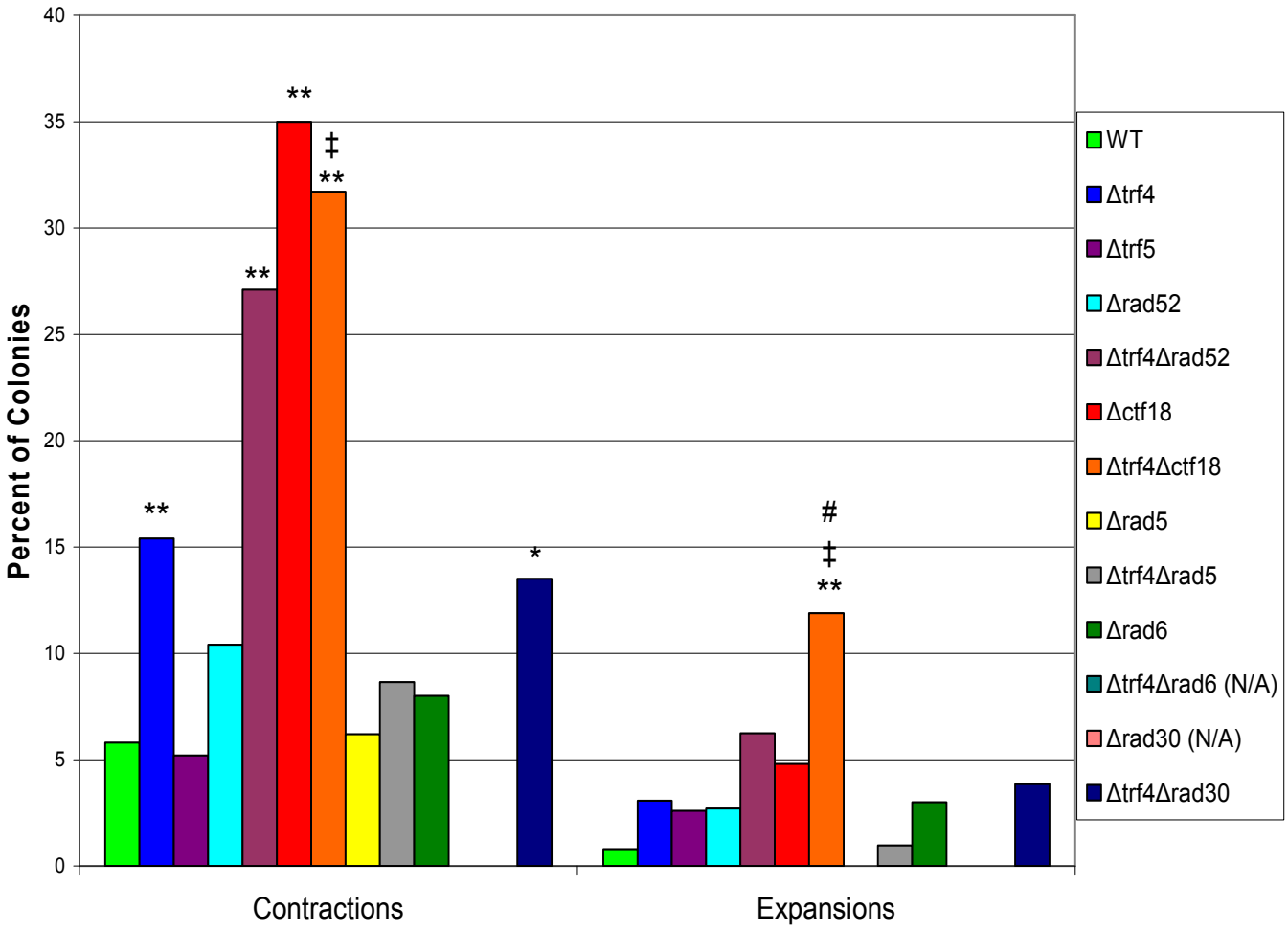

Appendix E: Instability Data for Δ*trf4*Δ*rad52* and Δ*trf4*Δ*ctf18*. The * symbol indicates $p<0.05$ in comparison to the wild-type, and ** indicates $p<0.01$ (Fischer's Exact Test). ‡ denotes a significant difference from Δ*trf4*, while # denotes a significant difference from the other single mutant (Fischer's Exact Test).

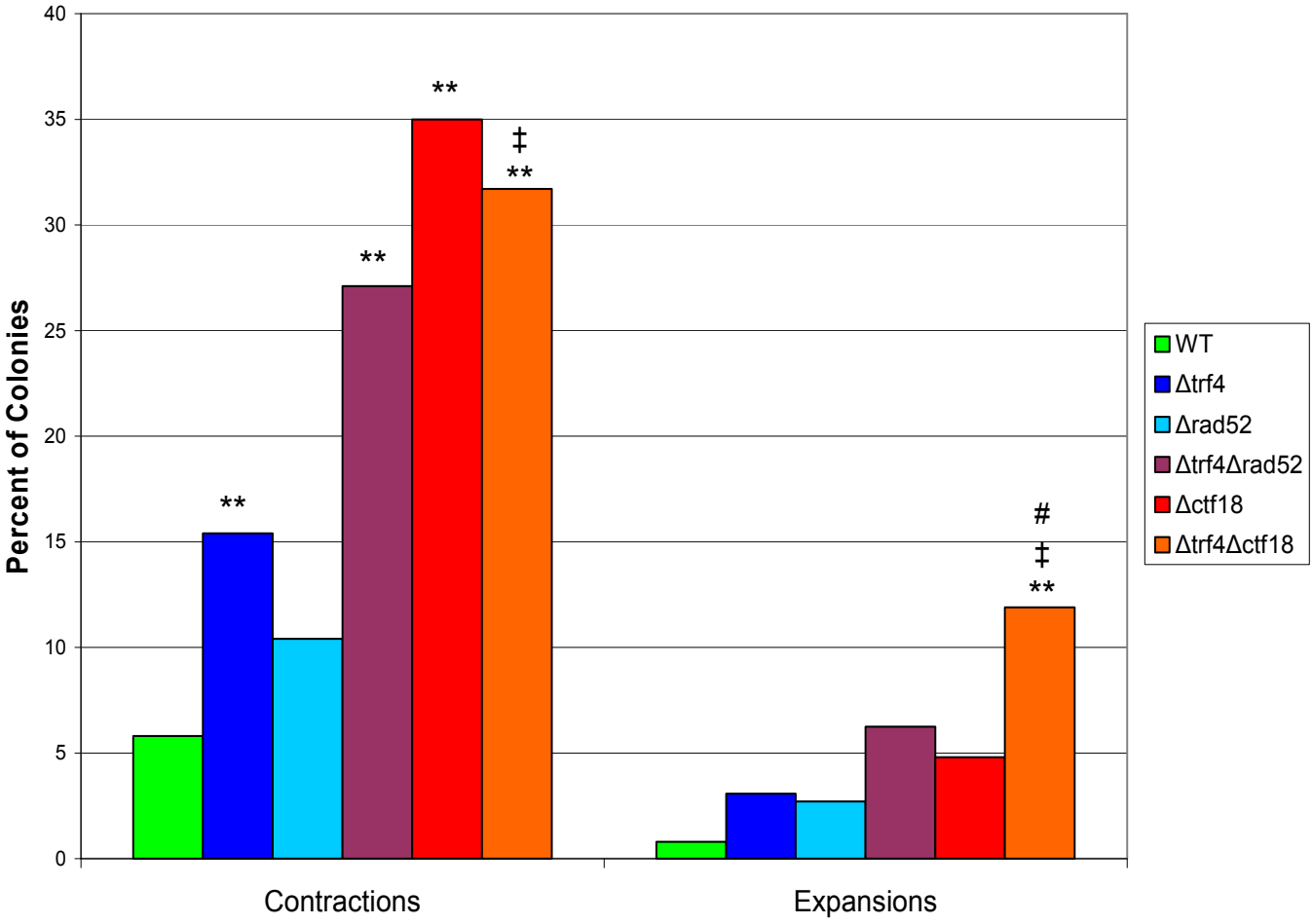

Appendix F: Instability Data for Postreplication Repair Mutants. The * symbol indicates $p<0.05$ in comparison to the wild-type, and ** indicates $p<0.01$ (Fischer's Exact Test). ‡ denotes a significant difference from Δ*trf4*, while # denotes a significant difference from the other single mutant (Fischer's Exact Test).